Applied Geochemistry 101 (2019) 109–126

Contents lists available at ScienceDirect

Applied Geochemistry

journal homepage: www.elsevier.com/locate/apgeochem

A multi-instrumental geochemical approach to assess the environmental impact of CO_2-rich gas emissions in a densely populated area: The case of Cava dei Selci (Latium, Italy)

S. Venturi[a,b,*], F. Tassi[a,b], J. Cabassi[a], O. Vaselli[a,b], I. Minardi[c], S. Neri[c], C. Caponi[b], G. Capasso[d], R.M.R. Di Martino[d], A. Ricci[e], F. Capecchiacci[b], M. Lelli[f], A. Sciarra[g], D. Cinti[g], G. Virgili[c]

[a] Institute of Geosciences and Earth Resources (IGG), National Research Council of Italy (CNR), Via G. La Pira 4, 50121, Florence, Italy
[b] Department of Earth Sciences, University of Florence, Via G. La Pira 4, 50121, Florence, Italy
[c] West Systems Co. Ltd, Via Don Mazzolari 25, 56025, Pontedera, Italy
[d] Istituto Nazionale di Geofisica e Vulcanologia, Sezione di Palermo, Via Ugo La Malfa 153, 90146, Palermo, Italy
[e] Department of Biological, Geological and Environmental Sciences, University of Bologna, Porta S. Donato 1, 40136, Bologna, Italy
[f] Institute of Geosciences and Earth Resources (IGG), National Research Council of Italy (CNR), Via G. Moruzzi 1, 56124, Pisa, Italy
[g] National Institute of Geophysics and Volcanology (INGV), Via di Vigna Murata 605, 00143, Rome, Italy

ARTICLE INFO

Editorial handling by Dr T. H. Darrah

Keywords:
CO_2 diffuse degassing
Air quality
Cava dei Selci
Colli Albani
Gas hazard

ABSTRACT

The Colli Albani volcanic complex (Lazio, Italy) hosts areas characterized by anomalously high emissions of CO_2-rich gases (e.g. Tivoli, Cava dei Selci, Tor Caldara, Solforata). The source of these gases is a regional aquifer within the Mesozoic carbonate rock sequences. These degassing zones release significant concentrations of H_2S and other toxic gases (e.g. GEM: Gaseous Elemental Mercury, and Rn) and represent a serious hazard for local inhabitants, especially for those living at Cava dei Selci (near Rome, Italy), where the emitting areas are nested inside residential neighborhoods. In April 2016, a comprehensive geochemical survey was carried out in an abandoned stone quarry nearby the urban settlement aimed to: (i) investigate the gas composition from both punctual discharges and anomalously high diffuse soil degassing sites, and (ii) evaluate their environmental impact on the local air quality. The spatial distribution of the soil CO_2 fluxes was mainly dependent on the local geostructural setting, whereas shallow secondary processes (e.g. oxidation and gas-water interaction) likely represent the main controlling factor on reactive and/or water-soluble gas species, such as CH_4 and H_2S. The total output of CO_2 from the abandoned stone quarry accounted for 0.53% of total CO_2 discharged from the whole Colli Albani volcanic district. The naturally emitted toxic gases (e.g. CO_2, H_2S, CH_4, GEM) largely affect the air quality and pose a serious threat for the health of the local residents. A mobile multi-instrumental station able to continuously and simultaneously acquire CO_2, H_2S, SO_2, CH_4, GEM and CO was deployed to verify the concentrations of both the main deep-originated gas compounds and potential secondary gaseous contaminants (i.e. SO_2) around and inside the urban settlement most exposed to the lethal gases. Hydrogen sulfide was found to be the most impacting gas, occasionally exceeding the 24-h air quality guideline for ambient air and causing odor annoyance at a distance up to more than 250 m downwind from the emitting area. In poorly ventilated basements, toxic gas accumulations up to hazardous levels were measured, producing anomalous outdoor air concentrations at the street level in front of the descending vehicular access to private garages and relatively far from the main emitting area. The geochemical survey, carried out via mobile station and soil gas measurements, resulted to be particularly efficient for evaluating the potential effects caused by gas emissions in inhabited areas. The multi-measurement approach adopted in the present study is of paramount importance for managing future urban development plans.

1. Introduction

Geogenic CO_2-rich gas emissions discharge from large sectors of the peri-Tyrrhenian segment in central and southern Italy (i.e. southern Tuscany, Latium and Campania; Chiodini et al., 2000, 2004; Chiodini, 2008; Chiodini et al., 2013), where degassing areas are favored by (i)

* Corresponding author. Institute of Geosciences and Earth Resources (IGG), National Research Council of Italy (CNR), Via G. La Pira 4, 50121, Florence, Italy.
E-mail address: stefania.venturi@igg.cnr.it (S. Venturi).

https://doi.org/10.1016/j.apgeochem.2019.01.003
Received 2 March 2018; Received in revised form 4 January 2019; Accepted 4 January 2019
Available online 07 January 2019
0883-2927/

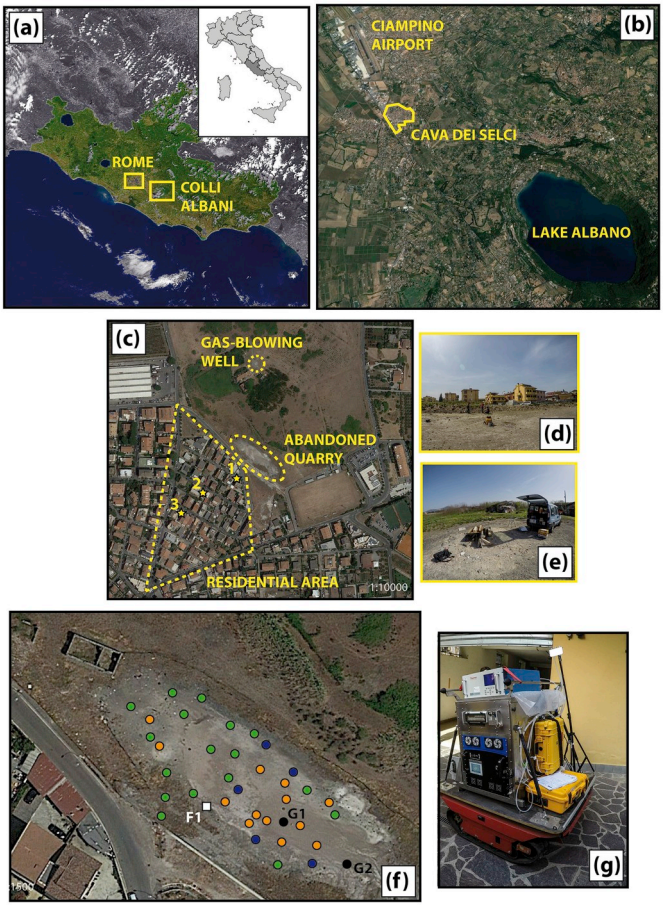

Fig. 1. (a) Satellite image of Latium (Italy) with the location of Colli Albani and Rome. (b) Satellite image of the Colli Albani area, from Ciampino airport to Lake Albano. The location of Cava dei Selci is reported. (c) Satellite image of Cava dei Selci. The emitting areas from the abandoned stone quarry and the gas-blowing well are countered with a dashed yellow line, together with the residential area where real-time continuous measurements of air quality were performed. The location of the windowless garage, the aerated garage and the descending vehicular access to a private garage are indicated with yellow stars (labeled 1, 2, and 3, respectively). (d) Photograph of the abandoned stone quarry in front of the houses of Cava dei Selci. (e) Photograph of the gas-blowing well and the fixed measuring station at F2 for air quality measurements. (f) Location of the sampling sites where the puncutal gas emissions (G1 and G2; black circles) and interstitial soil gases (*A* soil gases: orange circles; *B* soil gases: green circles; *C* soil gases: blue circles) were collected and position of the fixed measuring station for air quality measurements (F1; white square) in the abandoned stone quarry. (g) Photograph of the mobile prototype for real-time continuous measurements of air quality. (For interpretation of the references to colour in this figure legend, the reader is referred to the Web version of this article.)

crustal thinning (< 25 km; Scrocca et al., 2003), (ii) seismic activity (Frepoli and Amato, 1997; Mariucci et al., 1999; Chiodini et al., 2004 and references therein), (iii) high heat flow (up to 200 mW/m^2; Cataldi et al., 1995) and (iv) Quaternary volcanism. The latter formed a NW-SE-aligned sequence of volcanic complexes (Mattei et al., 2010) that also includes Colli Albani (Fig. 1a). This volcanic system is considered in a quiescent period (Carapezza et al., 2012; Marra et al., 2016), although Trasatti et al. (2018) suggested a rejuvenation of the Colli Albani magmatic system based on deformation modelling and helium isotopic signature in local gas manifestations. The volcanic complex, that hosts a 175 m deep lake (e.g. Cioni et al., 2003; Carapezza et al., 2008; Barbieri et al., 2013; Cabassi et al., 2013), is at about 20 km SE of Rome (Latium, Central Italy; Fig. 1a) and is located in one of the most densely populated municipalities of Latium. Permanent gas (mainly consisting of CO_2 and H_2S) emissions (e.g. Hooker et al., 1985; Giggenbach et al., 1988; Minissale, 2004; Carapezza et al., 2012) dot the whole area. The total CO_2 discharged from the Colli Albani volcanic district was estimated to be higher than 4.2×10^9 mol/y (Chiodini and Frondini, 2001). Sudden gas leakages from CO_2 oversaturated ground waters are often documented (Chiodini and Frondini, 2001; Annunziatellis et al., 2003; Carapezza and Tarchini, 2007). The gas manifestations frequently occur in close proximity to residential settlements, arousing severe environmental concern about possible human health risks related to both short- and long-term exposure to the discharged gaseous compounds. Being denser than air, CO_2 and H_2S may accumulate in topographic depressions and house basements up to hazardous levels (Annunziatellis et al., 2003; Beaubien et al., 2003; Carapezza et al., 2003, 2012). Carbon dioxide has severe health effects on humans and animals (e.g. rapid breathing and heart rate, headache, nausea and vomiting, collapse, convulsions, and even coma and death) at high concentrations (e.g. Gellhorn, 1936; Sechzer et al., 1960; Langford, 2005). The immediately dangerous to life or health (IDLH) value established by the National Institute for Occupational Safety and Health (NIOSH) is of 72,000 mg/m^3 (NIOSH, 1996; Department of Health and Human Services (NIOSH), 2007). Consequently, few minutes of exposure at 126,000–180,000 mg/m^3 causes unconsciousness (NIOSH, 1996). H_2S levels > 450 mg/m^3 can induce, in order of increasing concentration: pulmonary edema, strong central nervous system stimulation, hyperpnoea followed by respiratory arrest, immediate collapse with respiration paralysis (WHO, 2000). The lowest-observed-adverse-effect level (LOAEL) of H_2S is 15 mg/m^3, when eye irritation occurs, although a lower threshold (2.8 mg/m^3) was recognized for respiratory effects in asthmatics (WHO, 2003 and references therein). Besides CO_2 and H_2S, several other toxic species are present at hazardous concentrations in the gases discharged from Colli Albani. For instance, Beaubien et al. (2003) measured anomalously high concentrations of Rn in soil gases (> 250 kBq/m^3), exposing the residents to a long-term risk of developing lung cancer (Dubois, 2005).

One of the most important and impressive degassing sites at Colli Albani is located in an abandoned stone quarry at the northeastern edge of the town of Cava dei Selci (Fig. 1b), 20 m away from buildings and houses. Endogenous gases are discharged both from punctual emissions and through diffuse soil degassing in such a huge amount that the surrounding air occasionally becomes almost unbreathable up to even 2 m above the ground level (Pizzino et al., 2002; Carapezza et al., 2003 and references therein). Moreover, gas tends to permeate and accumulate into the nearby basements and ground floors, frequently causing hazardous indoor concentrations of CO_2 and H_2S. Occasionally, local Authorities are forced to evacuate the residents when the meteorological conditions favor the increment of the noxious gases (Carapezza and Tarchini, 2007; Carapezza et al., 2012). The degassing area of Cava dei Selci and the related gas hazard were studied in detail by several authors, who mainly focused on specific intradisciplinary issues, such as (i) unraveling the origin of gas emissions (e.g. Giggenbach et al., 1988), (ii) estimating the total output of CO_2 and H_2S from the abandoned quarry (e.g. Chiodini and Frondini, 2001), (iii) measuring air concentrations of CO_2 and H_2S in the emitting area (e.g. Carapezza et al., 2012), and (iv) determining soil gas concentrations of specific toxic compounds (e.g. Rn; Beaubien et al., 2003). Nevertheless, a deeper understanding of the complex environmental issues at Cava dei Selci requires a multidisciplinary approach to provide a more holistic comprehension of the impact of natural gas emissions on air quality and human health and reliable information for the definition of intervention plans.

As a consequence, a complete characterization of the Cava dei Selci gases should consider both punctual gas emissions and interstitial soil gases, whose composition can significantly be modified by secondary chemical-physical (e.g. oxidation reactions, vapor condensation, interactions with shallow aquifers; e.g. Tassi et al., 2013) and biochemical (e.g. Huber et al., 2000; Norris et al., 2002; Glamoclija et al., 2004;

Henson et al., 2005; D'Alessandro et al., 2011; Gagliano et al., 2014; Tassi et al., 2015a,b) processes, which govern the release of gaseous compounds at the air-soil interface.

Once emitted in the atmosphere, gases are dispersed according to: (i) output rate from the emitting source(s), (ii) meteorological parameters (e.g. wind speed and direction, air humidity and temperature), (iii) physical properties of each gas species (e.g. molecular weight), and (iv) chemical reactions affecting the different gas species as a function of their reactivity. A fixed monitoring station may not be able to acquire all the necessary information to characterize a certain area affected by air contamination (e.g. Peralta et al., 2013; Olafsdottir et al., 2014). Consequently, mobile measurement platforms (e.g. Kolb et al., 2004) are an interesting and reliable alternative since they are set to obtain large datasets of air pollutants within and in the surroundings of a specific area to (i) gather information about the role played by the environmental parameters and chemical processes on air quality (e.g. Cabassi et al., 2017 and references therein), (ii) recognize areas more prone to hazardous gases, and (iii) select the best sites to locate fixed measuring stations.

In this paper, the abandoned stone quarry at Cava de Selci and surrounding areas were the sites where we adopted a multidisciplinary strategy, which included direct and remote measurements, aimed to (i) chemically and isotopically characterize the gases released from punctual discharges and those permeating the soil at shallow depths, (ii) measure soil CO_2, H_2S and CH_4 fluxes, and iii) determine the concentrations of CO_2, H_2S, SO_2, CH_4, GEM and CO in air at the stone quarry and the residential area from both outdoor and indoor environments. The field survey was carried out at Cava dei Selci from the 5th to the 6th of April 2016.

2. Study area

Cava dei Selci is an intensely urbanized area in the municipality of Marino (ca. 43,500 inhabitants), close to the Ciampino International Airport (Rome, central Italy). It is located on the NW side of Colli Albani (Fig. 1a,b), a quiescent alkali-potassic volcanic district (Trigila et al., 1995; Peccerillo, 1999, 2005; Giordano et al., 2006; Carapezza et al., 2010) characterized by a low-to-medium-enthalpy CO_2-rich fluid reservoir (Giggenbach et al., 1988) that is part of a regional aquifer (e.g. Chiodini et al., 1999) hosted in the structural highs of the Mesozoic carbonates overlying a Paleozoic metamorphic basement (e.g. Orlando et al., 1994). The origin of CO_2 was ascribed to (i) metamorphic reactions involving carbonate formations and (ii) mantle degassing (Giggenbach et al., 1988; Rogie et al., 2000; Chiodini and Frondini, 2001; Minissale, 2004; Carapezza and Tarchini, 2007; Iacono Marziano et al., 2007). Nitrogen, H_2S and CH_4 are minor constituents of the gases emitted from the area (Annunziatellis et al., 2003; Chiodini and Frondini, 2001; Carapezza et al., 2003), as well as the short-lived Rn isotopes, whose presence suggests that fluids rise quite rapidly through high permeable pathways, i.e. faults and fractures (Beaubien et al., 2003). Cava dei Selci lies on the north-western margin of the NE volcanotectonic active structure bordering the Ciampino horst, a NW-SE-oriented structural high of the Mesozoic carbonate basement (Amato and Chiarabba, 1995; Di Filippo and Toro, 1995; Carapezza et al., 2003), where one of the main degassing sites of the Colli Albani volcanic complex is located. It consists of a 10,000 m^2 wide area located close to residential buildings (Fig. 1c and d). Until the 1970s, the site was a stone quarry. The excavation removed the superficial low permeability volcano-sedimentary cover and formed a depression that was filled with loose material after the closure of the quarry. The highly permeable filling deposits were progressively altered by the uprising acidic fluids, and turned to be clay-rich (Carapezza et al., 2003, 2012; Carapezza and Tarchini, 2007). A stagnant water pool emerges at the bottom of the depression during the rainy season (November to March) and disappears in the summer period (June to September). The gas is released both diffusively from the soil and through punctual vents, the latter forming bubbling pools in the rainy season (Carapezza et al., 2003). Less than 200 m north of the degassing area, a dry gas emitting old water well (Fig. 1c,e) is present. It is reported that a gas blast likely occurred in the recent past as happened for other wells in the region (Carapezza and Tarchini, 2007; Carapezza et al., 2010).

In the abandoned quarry, lethal concentrations of both CO_2 and H_2S were occasionally measured by Carapezza et al. (2010, 2012) at ≤ 1 m height above the ground, particularly at dawn when wind ceases to blow. Several lethal accidents caused by gas inhalation occurred in the area, involving both humans (a man died in December 2000) and animals (29 cows in 1999, a sheep in March 2000 and 3 sheep in 2001 were asphyxiated; Annunziatellis et al., 2003; Carapezza et al., 2003). An exhaustive solution to the problem is far from being achieved by risk stakeholders, notwithstanding the insistent recommendations based on outdoor and indoor measurements of toxic gases, clearly highlighting the strong risks posed by these natural gas emissions (e.g. Beaubien et al., 2003; Carapezza et al., 2003, 2010, 2012). After the installation of a CO_2 measurement station that was prematurely dismissed, the main emission zone, i.e. the old quarry, was only temporary fenced with some wire mesh.

3. Materials and methods

3.1. Sampling and analytical methods for gases

3.1.1. Sampling procedures

Gases from two punctual gas vents (G1 and G2; Fig. 1f) and the gas-blowing well (G3) (Fig. 1c,e) were collected into (i) two-way Pyrex bottles, for the analysis of the $^{13}C/^{12}C$ ratios of CO_2 and CH_4 and the isotope compositions of He and Ar, (ii) pre-evacuated 60 mL glass flasks, equipped with Teflon stopcocks and filled with 20 mL of a 4 M NaOH solution, for determination of the chemical composition (Vaselli et al., 2006) and (iii) 30 mL glass bottles equipped with two stopcocks for measuring H_2 and CO. At each sampling point, a fourth aliquot for the analysis of the organic gases was collected into a 12 mL glass vial equipped with a pierceable rubber septum (Labco Exetainer®) (Tassi et al., 2015a).

Interstitial soil gases were collected from 35 sites in the abandoned stone quarry (Fig. 1f) using 12 mL glass vials and a 1 m long stainless steel tube (Tassi et al., 2015a) inserted at 20 or 10 cm depth. The shallowness of the water table or the soil hardness prevented to go deeper.

3.1.2. Analytical techniques

Inorganic gases in both the headspace of the 60 mL glass flasks (N_2, O_2 + Ar, Ne, and He) and the 12 mL glass vials (N_2, O_2 + Ar) were analyzed using a Shimadzu 15A gas chromatograph (GC) equipped with a thermal conductivity detector (TCD) and a 10 m long 5A Molecular Sieve column and He or Ar as gas carrier. Carbon dioxide and H_2S in the glass vials were analyzed using the same GC equipped with a 3 m long column packed with Porapak Q 80/100 mesh and He as gas carrier. Argon and O_2 peaks were efficiently separated using a Thermo Focus gas chromatograph equipped with a 30 m long capillary molecular sieve column and a TCD. Hydrogen and CO were measured in the 30 mL glass bottles using a Carlo Erba GC, equipped with a Reductant Gas Detector (RGD) and 5 m long 5A Molecular Sieve packed column.

The alkaline solution in the glass flasks was used for the analysis of (i) CO_2, as CO_3^{2-} by acidimetric titration (AT) with 0.5 N HCl solution, and (ii) H_2S, as SO_4^{2-} by ion chromatography (IC) after oxidation with H_2O_2 (Montegrossi et al., 2001; Vaselli et al., 2006).

Light hydrocarbons ($C_{\leq 3}$) were analyzed using a Shimadzu 14A gas chromatograph equipped with a Flame Ionization Detector (FID) and a 10 m long stainless steel column packed with Chromosorb PAW 80/100 mesh coated with 23% SP 1700. The heavier Volatile Organic Compounds (VOCs) were analyzed by GC (Thermo Trace Ultra) coupled to a Thermo DSQ Quadrupole Mass Spectrometer (MS) after extraction

using the Solid Phase Micro Extraction (SPME; Arthur and Pawliszyn, 1990) technique. The SPME was carried out using a 2 cm long three-phase fiber made of DiVinylBenzene (DVB) – Carboxen (Car) – Poly-DiMethylSiloxane (PDMS) (Supelco; Bellefonte, PA, USA). In the laboratory, the fiber was introduced into the glass vials through the porous membrane using a manual SPME device and exposed to the sampled gases for 30 min at 20 °C. Then, the VOCs absorbed into the SPME fiber were desorbed for 2 min at 230 °C in the column headspace of the GC-MS. The desorbed gases were injected through a port operating in splitless mode and equipped with a SPME liner (0.75 mm inner diameter) into a 30 m × 0.25 mm (1.4 μm inner diameter) film thickness TR-V1 fused silica capillary column (Thermo), using He as carrier gas at a flow rate of 1.3 mL/min in constant pressure mode. The column oven temperature was set, as follows: 35 °C (hold 10 min), ramp at 5.5 °C/min to 180 °C (hold 3 min), ramp at 20 °C/min up to 230 °C (hold 6 min). After the chromatographic separation, gases passed through a transfer-line set at 230 °C to the MS operating in positive electron impact mode (EI), with an ionization energy of 70 eV and a source temperature of 250 °C. A mass range from 35 to 400 m/z in full scan mode was analyzed. Retention times of the chromatographic peaks and the mass spectra were both used to identify VOCs detected by the quadrupole detector, using the mass spectra database of the NIST05 library (NIST, 2005) for comparison. Quantitative analyses were carried out by external standard calibration procedure using Accustandard® mixtures in methanol or, alternatively, hexane solvent. Relative Standard Deviation (RSD), calculated from five replicate analyses of the standard mixtures, was < 5%. The limit of quantification (LOQ) was determined by linear extrapolation from the lowest standard in the calibration curve using the area of a peak having a signal/noise ratio of 5. Analytical errors for GC, AT and IC were < 5%.

Gas samples for noble gas isotopic analyses were purified in high-vacuum line with cryogenic traps (10 K) directly connected to the mass spectrometer. The $^{3}He/^{4}He$ ratios were measured by a Helix SFT-GVI double collector and ^{40}Ar, ^{38}Ar, $e^{36}Ar$ by a Helix MC-GVI mass spectrometer. Calibration for measurements of isotope abundances of He and Ar were performed using atmospheric standards. The analytical errors for He and Ar isotope analyses were ≤0.3% and ≤0.1%, respectively.

The $^{13}C/^{12}C$ ratios of CO_2 (expressed in ‰ vs. V-PDB) were measured with a Thermo Delta V Plus dual inlet mass spectrometer after purification of the gas mixture by standard procedures using cryogenic traps (Evans et al., 1998; Vaselli et al., 2006; Paonita et al., 2012). Calibration was performed by using a standard prepared by quantitative reaction of certified Carrara Marble ($\delta^{13}C_{MAB}$ = +2.45‰ vs. V-PDB) with anhydrous phosphoric acid (H_3PO_4).

The isotopic analysis $^{13}C/^{12}C$ of CH_4 was performed using a Delta Plus XP IRMS equipped with a Thermo TRACE GC interfaced with Thermo GC/C III. Thermo TRACE gas chromatograph was equipped with a Poraplot-Q column. The injection system is better described in Grassa et al. (2010). CH_4 was quantitatively converted to CO_2 by passing through a combustion oven (T = 940 °C). The $^{13}C/^{12}C$ ratios are reported as $\delta^{13}C$ values against V-PDB standard. The uncertainties of measurements are ± 0.15‰.

3.2. Soil flux measurements

Soil fluxes of CO_2, CH_4 and H_2S were measured at 81 sites in the abandoned stone quarry using the "accumulation chamber" (AC) method (Chiodini et al., 1998). The measurements were performed using West Systems Co. Ltd. portable flux meters, consisting of (i) an inverted chamber (a cylindrical metal vase with a basal area of 200 cm^2 and an inner volume of 3060 cm^3), (ii) CO_2, CH_4 or H_2S gas detectors, (iii) an analog-to-digital (AD) converter, and (iv) a palmtop computer. The AC detectors consist of (i) an Infra-Red (IR) spectrophotometer (Licor® Li-820, measurement range and accuracy: 0–36,000 mg/m^3 and 4%, respectively) for CO_2, (ii) a detector based on tunable diode laser absorption spectroscopy (TDLAS) combined with a Herriot multipass cell for CH_4, and (ii) an electrochemical detector for H_2S. Once the chamber was firmly placed on the ground, the soil gas was continuously pumped from the chamber, using a low-flux pump (20 mL/s), to the IR spectrophotometer, and then injected back into the chamber to minimize the disturbance on the gas flux. The gas flux from the soil (Φi, where i is CO_2, CH_4 or H_2S) was then determined, according to the following equation (Chiodini et al., 1998):

$$\phi_i = cf \times dC_i/dt \quad (1)$$

where cf is the proportionality factor between the increase in time of the gas concentrations inside the chamber (dC_i/dt) and Φi, which depends on the geometry of the measuring equipment (Chiodini et al., 1998). The lower detection limits (d.l.) for ΦCO_2, ΦCH_4 and ΦH_2S were ~0.08, ~0.008 and ~0.00348 g m^{-2} day^{-1}, respectively. For statistical analysis, values below d.l. were replaced by d.l./2.

The probability distribution analysis of flux data and the estimation of the total CO_2, CH_4 and H_2S output from the study area was performed through the graphical statistical approach (GSA) method described by Chiodini et al. (1998), while the sequential Gaussian simulations (sGs) approach was applied in order to produce a map of CO_2 diffuse degassing (Deutsch and Journel, 1998; Cardellini et al., 2003, 2017; Frondini et al., 2004).

3.3. Measurements of air pollutants

Air pollutants were determined (i) at two fixed measuring stations, located in the abandoned stone quarry (F1; Fig. 1f) and close to the gas-blowing well (F2; Fig. 1c,e), respectively, and (ii) along the streets and inside two private garages in the residential area (Fig. 1c) using a Mobile Multi-instrumental Station (MMS; Fig. 1g). The sites where the fixed stations were installed and the measuring pathways throughout the town were digitalized using a portable GPS (Garmin® GPSMAP 62), whilst the meteorological parameters (wind speed and direction) were measured with a Davis® Vantage Vue weather mobile station placed within the study area. The measured air pollutants were, as follows: CO_2, H_2S, SO_2 and GEM (Gaseous Elemental Mercury). The $\delta^{13}C$-CO_2 values at the fixed stations and the concentrations of CO and CH_4 via the mobile station were also measured.

3.3.1. Fixed measuring stations

At F1 and F2 the measurements were performed at 1 and 0.25 m above the ground, respectively. The instruments were placed downwind of the emitting area and the gas-blowing well, respectively.

The air concentrations of sulfur-bearing inorganic gases (H_2S and SO_2) were determined using a Thermo® 450i analyzer featuring a pulsed fluorescence technology. The air is pumped at 1 L/min into the analyzer and directed to either (i) a converter, where H_2S is oxidized to SO_2 (efficiency > 80%) or (ii) the fluorescence chamber, i.e. bypassing the converter. In the fluorescence chamber, pulsating UV light excites the SO_2 molecules. As the excited SO_2 molecules decay to lower energy states, they emit a UV light, detected by a photomultiplier tube (PMT), whose intensity is proportional to the SO_2 concentration. When the air sample passes through the converter, the instrument measures the concentrations of Combined Sulfur (CS), i.e. the sum of SO_2 and H_2S. When the air flux bypasses the converter, the analyzer only determines SO_2. The H_2S content is then calculated as the difference between the two signals (Thermo Fisher Scientific, 2012). The instrument provides concentrations by averaging the measurements carried out each 60s (precision ± 1%; Thermo Fisher Scientific, 2012). The detection limits were 5.2 and 2.8 μg/m^3 for SO_2 and H_2S, respectively (Thermo Fisher Scientific, 2012). During the field surveys, the instrumentation was power-supplied by a high-performance portable gel battery.

GEM air concentration measurements were performed using a Lumex® RA-915M analyzer, i.e. a portable atomic absorption spectrometer with Zeeman background correction for interference-free

measurements combined with high frequency modulation of polarized light. The radiation source (Hg lamp) is placed in a permanent magnetic field, whereby the 254 nm mercury resonance line is split into three polarized components, two of which are detected for the analysis. After passing through a polarization modulator, the radiation reaches a multi-path cell that isolates the 254 nm resonance line allowing high selectivity and sensitivity (Sholupov and Ganeyev, 1995; Sholupov et al., 2004). The instrument operates at a flow rate of 10 L/min and is supplied by a rechargeable internal battery allowing up to 8 h of continuous measurements. The detection limit was 2 ng/m^3 while the accuracy of the method was 20% from 2 to 50,000 ng/m^3 (Sholupov and Ganeyev, 1995; Sholupov et al., 2004). For the present study, the measurement acquisition frequency was of 1 s and GEM data were averaged over 1 min to be coupled with those of H_2S and SO_2.

Concentration and isotopic composition of CO_2 in air were determined using a Thermo Scientific Delta Ray™ Isotope Ratio Infrared Spectrometer (IRIS) analyzer. The instrument is equipped with a tunable diode laser operating at a mid-infrared wavelength (4.3 μm) employing a simple and direct absorption approach using a path length of only 5 m. The analyzer works at ambient CO_2 over the concentration range of 360–6300 mg/m^3 and high precision is achieved using gas standard for calibration at known CO_2 concentration and isotope composition every 20 min. The sampling frequency of the detector signal is recorded at 1 Hz, and the $\delta^{13}C_{(CO2)}$ values were averaged over a time interval of 60 s of stable acquisition.

The isotope composition of carbon was expressed as $\delta^{13}C$-CO_2‰ versus V-PDB. The adopted measurement method allowed to achieve precision for $\delta^{13}C_{(CO2)}$ of ± 0.15‰ (Di Martino et al., 2016).

3.3.2. Mobile multi-instrumental station (MMS)

The MMS is a prototype developed by West Systems Co. Ltd (Laville et al., 2015) for real-time continuous monitoring of air quality. The traction system (Fig. 1g) includes a self-propelled crawler machine equipped with two engines and the respective electronic controllers. The battery pack of the crawler machine, coupled with an inverter of 24 VDC input, provides AC (alternating current) power (up to 1500 W) to the instruments (Laville et al., 2015).

The gas analyzers set on the MMS was composed by 4 modules, as follows: (i) Thermo® 450i analyzer, (ii) Lumex® RA-915M analyzer, (iii) Los Gatos Research Ultraportable Greenhouse Gas Analyzer (LGR-UGGA) for CO_2 and CH_4, and (iv) Los Gatos Research LGR 913-0015 analyzer for CO. The inlet tubes of the instruments were fixed to a mast installed on the MMS allowing to convey air samples from ~1.80 m above the ground.

The LGR UGGA and LGR 913-0015 gas analyzers are spectrometers using Los Gatos Research's patented off-axis ICOS (integrated cavity output spectroscopy) technology, a fourth-generation cavity. They require 60 W (powered with 10–30 VDC) and 300 W (powered with 230 VAC), respectively. The measurement range of LGR UGGA was from 1 to 36,000 mg/m^3 and from 0.007 to 66 mg/m^3 for CO_2 and CH_4, respectively, whilst the linear dynamic range of LGR 913-0015 was from 0.006 to 4.58 mg/m^3.

4. Results

4.1. Chemical and isotopic ($\delta^{13}C$-CO_2, $^{40}Ar/^{36}Ar$ and R_c/R_a) composition of gas emissions

The chemical and isotopic composition of gases emitted from (i) the two punctual vents (G1 and G2; Fig. 1f) and (ii) the gas-blowing well (G3; Fig. 1c,e) are reported in Table 1. The chemical composition of the inorganic gas fraction was largely dominated by CO_2 (with concentrations ranging from 982 to 990 mmol/mol), followed by H_2S (from 5.6 to 11 mmol/mol). The concentrations of N_2 varied from 3.2 to 5.6 mmol/mol, whilst O_2 and Ar ranged from 0.087 to 0.13 and from 0.026 to 0.051 mmol/mol, respectively. Methane had concentrations between 0.68 and 0.91 mmol/mol, while those of H_2 and CO ranged from 0.015 to 0.056 and from 0.0009 to 0.0033 mmol/mol, respectively. Helium and Ne were up to 0.0011 and 0.000078 mmol/mol, respectively.

Table 1
Chemical and isotope compositions of gases emitted from punctual gas emissions at Cava dei Selci. The concentrations of inorganic gas species and methane are expressed in mmol/mol, whilst the contents of organic compounds are reported in μmol/mol. The $\delta^{13}C$ values of CO_2 and CH_4 are expressed in delta (δ) per mil (‰) against Vienna Pee Dee Belemnite (V-PDB).

	G1	G2	G3
CO_2 (mmol/mol)	985	982	990
H_2S (mmol/mol)	9.2	11	5.6
N_2 (mmol/mol)	4.3	5.6	3.2
O_2 (mmol/mol)	0.13	0.087	0.095
Ar (mmol/mol)	0.032	0.051	0.026
Ne (mmol/mol)	0.000078		0.000013
He (mmol/mol)	0.0011		0.0011
H_2 (mmol/mol)	0.036	0.056	0.015
CO (mmol/mol)	0.0033	0.0009	0.0013
CH_4 (mmol/mol)	0.82	0.91	0.68
$d^{13}C$-CO_2 (‰ vs. V-PDB)	1.08	0.9	0.73
$D^{13}C$-CH_4 (‰ vs. V-PDB)	−29	−30	−32
R/R_a	1.40		1.41
R_c/R_a	1.41		1.41
$^{40}Ar/^{36}Ar$	293		299
$^{38}Ar/^{36}Ar$	0.19		0.19
C_2H_6 (μmol/mol)	3.3	3.6	2.5
C_3H_8 (μmol/mol)	0.51	0.66	0.44
iC_4H_{10} (μmol/mol)	0.16	0.15	0.21
nC_4H_{10} (μmol/mol)	0.22	0.18	0.25
C_{5+} alkanes (μmol/mol)	0.71	0.69	0.56
C_6H_6 (μmol/mol)	0.61	0.64	0.47
branched aromatics (μmol/mol)	0.64	0.78	0.61
kenotes (μmol/mol)	0.15	0.60	0.28
aldehydes (μmol/mol)	0.15	0.13	0.11
Esters + acids (μmol/mol)	2.4	2.1	1.8
S-substituted (μmol/mol)	1.7	2.5	3.9
others (μmol/mol)	0.24	0.39	0.11

The total content of VOCs ranged from 10.8 to 12.4 μmol/mol (Table 1). Alkanes were the most abundant species, with concentrations ranging from 4.0 to 5.3 μmol/mol, corresponding to 35–45% of the total organic fraction (ΣVOCs). The concentrations of ethane (C_2H_6, from 2.5 to 3.6 μmol/mol) were one order of magnitude higher than those of propane (C_3H_8, ≤0.66 μmol/mol), normal-butane (n-C_4H_{10}, ≤0.25 μmol/mol) and iso-butane (i-C_4H_{10}, ≤0.21 μmol/mol) and long-chain C_{5+} alkanes (≤0.71 μmol/mol). S-substituted compounds were relatively abundant, ranging from 1.7 to 3.9 μmol/mol (i.e. from 16 to 35 %ΣVOCs). O-bearing species included esters + acids (from 1.8 to 2.4 μmol/mol), ketones (from 0.15 to 0.60 μmol/mol) and aldehydes (from 0.11 to 0.15 μmol/mol), corresponding to 19 up to 25% of the organic gas fraction. Among aromatics, C_6H_6 was the most abundant (from 0.47 to 0.64 μmol/mol) species, while the concentrations of branched aromatics ranged from 0.61 to 0.78 μmol/mol. On the whole, aromatics added up to 10–12% ΣVOCs.

The $\delta^{13}C$-CO_2 and $\delta^{13}C$- CH_4 values ranged from 0.73 to 1.08‰ vs. V-PDB and from −32 to −29‰ vs. V-PDB, respectively (Table 1), i.e. similar to those reported by previous studies (Giggenbach et al., 1988; Chiodini and Frondini, 2001; Annunziatellis et al., 2003; Carapezza and Tarchini, 2007; Carapezza et al., 2012).

The $^{40}Ar/^{36}Ar$ ratios (from 293 to 299; Table 1) were consistent with the atmospheric value (295.5). The measured isotopic composition of He was expressed as R/R_a, where R refers to the $^3He/^4He$ ratio in the sample and R_a is the $^3He/^4He$ ratio in the air (i.e. 1.4×10^{-6}). The measured R/R_a values (Table 1) were corrected for air contamination by using the He/Ne ratio, as follows:

Table 2
Chemical composition of main gas species (CO_2, H_2S, N_2, O_2, Ar, CH_4, in mmol/mol) and VOCs (in μmol/mol) in interstitial soil gas samples from Cava dei Selci.

ID	Depth	Type	CO_2 (mmol/mol)	H_2S (mmol/mol)	N_2 (mmol/mol)	O_2 (mmol/mol)	Ar (mmol/mol)	CH_4 (mmol/mol)	C_2H_6 (μmol/mol)	C_3H_8 (μmol/mol)	iC_4H_{10} (μmol/mol)	nC_4H_{10} (μmol/mol)	C_6H_6 (μmol/mol)	C_{5+} alkanes (μmol/mol)	Alkenes (μmol/mol)	branched aromatics (μmol/mol)	Kenotes (μmol/mol)	Aldehydes (μmol/mol)	carboxyl acids (μmol/mol)	Cyclics (μmol/mol)	S-substituted (μmol/mol)	Others (μmol/mol)
1	20	C	272		498	218	12	0.023	0.085	0.011	0.0023	0.0015	0.0014	0.008	0.011		0.0015	0.0011	0.0016	0.0018		
2	10	A	903	1.3	89	4.4	2.2	0.058	0.24	0.075	0.0088	0.0066	0.0054	0.076	0.056	0.00037	0.0074	0.0047	0.0065	0.0061	0.0007	0.0006
3	10	B	886	2.1	101	8.1	2.3	0.067	0.31	0.087	0.0091	0.0075	0.0074	0.091	0.069	0.00049	0.0023	0.0015	0.0026	0.0048	0.0009	0.0009
4	20	A	934	3.3	59	1.6	1.4	0.075	0.44	0.11	0.026	0.015	0.011	0.15	0.087	0.0012	0.016	0.013	0.011	0.012	0.0012	0.0011
5	20	A	928	3.2	66	1.2	1.6	0.044	0.21	0.061	0.011	0.0067	0.0069	0.045	0.048	0.00028	0.0026	0.0029	0.0033	0.0075	0.0011	
6	20	A	907	2.6	81	6.8	1.9	0.075	0.39	0.061	0.01	0.0055	0.006	0.041	0.044	0.00026	0.0033	0.0021	0.0036	0.0066	0.0006	0.0008
7	20	B	843	0.13	131	22	3.4	0.019	0.077	0.012	0.0021	0.0014	0.0012	0.0084	0.0071		0.0038	0.0036	0.0045	0.0015		
8	10	C	4.9		665	315	15	0.015	0.065	0.011	0.0018	0.0011	0.0012	0.0045	0.0036		0.0013	0.0008	0.0021	0.0011		
9	20	A	917	2.4	77	1.4	1.8	0.055	0.23	0.075	0.013	0.0077	0.0066	0.051	0.033	0.00027	0.0016	0.0011	0.0023	0.0054	0.0008	
10	20	A	913	1.9	81	1.5	1.9	0.13	0.61	0.15	0.026	0.015	0.012	0.16	0.11	0.0011	0.015	0.023	0.012	0.012	0.0005	0.0012
11	20	B	886	1.1	104	5.4	2.5	0.12	0.52	0.11	0.016	0.011	0.010	0.12	0.087	0.00085	0.011	0.16	0.011	0.012	0.0006	0.0008
12	20	C	19		671	295	15	0.026	0.095	0.014	0.0025	0.0018	0.0015	0.0061	0.0056		0.0018	0.0012	0.0022	0.0016		
13	20	A	928	0.88	66	3.6	1.6	0.036	0.18	0.032	0.0041	0.0016	0.0012	0.011	0.012		0.0026	0.0018	0.0034	0.0014		
14	20	A	944	1.9	51	1.5	1.4	0.11	0.56	0.096	0.012	0.0085	0.0078	0.088	0.076	0.00031	0.0055	0.0026	0.0058	0.0055	0.0007	0.0013
15	20	A	948	0.64	48	2.1	1.4	0.022	0.091	0.015	0.0023	0.0021	0.0015	0.012	0.015	0.00017	0.0021	0.0014	0.0025	0.0016		
16	20	A	920	0.14	76	2.3	1.8	0.025	0.11	0.023	0.0036	0.0041	0.0025	0.015	0.014	0.00019	0.0023	0.0015	0.0026	0.0027		
17	20	C	299		484	205	12	0.011	0.056	0.0095	0.0015	0.0011	0.0012	0.0011	0.0016		0.0008	0.0006	0.0011	0.0015		
18	20	A	962	0.39	36	0.51	0.85	0.098	0.47	0.086	0.0091	0.0075	0.0068	0.067	0.055	0.00023	0.0044	0.0021	0.0046	0.0069		0.0007
19	20	C	302		551	136	11	0.021	0.074	0.005	0.0005	0.0002	0.0002				0.0013	0.0005	0.0007	0.0005		
20	20	B	508		395	87	9.6	0.018	0.066	0.004	0.0006	0.0004	0.0003				0.0007	0.0005	0.0006	0.0004		
21	20	B	498		388	104	9.9	0.015	0.052	0.003	0.0005	0.0003	0.0002				0.0011	0.0005	0.0004	0.0006		
22	20	B	831	0.056	131	35	3.3	0.041	0.14	0.045	0.0094	0.0066	0.0045	0.033	0.025	0.00018	0.0041	0.00026	0.0054	0.0031		
23	20	B	846	0.22	125	26	3.1	0.034	0.13	0.042	0.0084	0.0051	0.0044	0.025	0.011	0.00015	0.0032	0.0017	0.0036	0.0039		
24	20	B	759	0.12	187	49	4.7	0.023	0.088	0.012	0.0018	0.0009	0.0005	0.0077	0.0055		0.0023	0.0012	0.0029	0.0006		
25	20	B	640	0.13	284	69	6.7	0.021	0.087	0.01	0.0016	0.0008	0.0007	0.0061	0.0033		0.0025	0.0017	0.0028	0.0008		
26	20	B	882	0.056	103	12	2.5	0.026	0.096	0.011	0.0015	0.0009	0.0008	0.0048	0.0025		0.0031	0.0016	0.0033	0.0007		
27	20	B	896	0.12	94	7.8	2.3	0.014	0.057	0.008	0.0009	0.0007	0.0006	0.0011	0.0016		0.0013	0.0006	0.0015	0.0005		
28	20	B	689	0.069	256	48	6.4	0.011	0.036	0.005	0.0007	0.0005	0.0006				0.0015	0.0008	0.0016	0.0003		
29	20	A	904	0.056	87	6.6	2.1	0.046	0.21	0.035	0.0066	0.0027	0.0039	0.026	0.012	0.00025	0.0024	0.0014	0.0021	0.0041		
30	20	B	876	0.46	115	5.1	2.8	0.054	0.28	0.049	0.0081	0.0035	0.0044	0.045	0.016	0.00039	0.0061	0.0038	0.0065	0.0026		0.0006
31	20	A	900	0.29	86	12	1.9	0.024	0.12	0.025	0.0051	0.0021	0.0036	0.014	0.0087	0.00011	0.0023	0.0012	0.0033	0.0035		
32	20	B	745	0.095	185	66	4.2	0.019	0.094	0.011	0.0016	0.0026	0.0021	0.0058	0.0011		0.0024	0.0013	0.0027	0.0026		
33	20	B	599	0.087	381	11	9.2	0.023	0.11	0.021	0.0066	0.0044	0.0035	0.016	0.012	0.00012	0.0036	0.0022	0.0033	0.0039		
34	20	B	744	0.11	215	36	4.7	0.021	0.085	0.015	0.0045	0.0039	0.0029	0.011	0.0076	8E-05	0.0021	0.016	0.0025	0.0025		
35	20	B	742	0.12	202	51	4.5	0.022	0.091	0.017	0.0051	0.0044	0.0035	0.012	0.0078	9E-05	0.0022	0.0015	0.0025	0.0037		

$$R_c/R_a = \frac{(R/R_a)(He/Ne)_m - (He/Ne)_a}{(He/Ne)_m - (He/Ne)_a} \quad (2)$$

where subscripts *m* and *a* refer to the values measured in samples and in air, respectively. The corrected R_c/R_a ratios were 1.41 in both G1 and G3 samples (Table 1).

4.2. Chemical composition of interstitial soil gases

The chemical composition of the interstitial soil gases is reported in Table 2. Concentrations of CO_2 and N_2 were highly variable (from 4.9 to 962 mmol/mol and from 36 to 671 mmol/mol, respectively) and inversely correlated. On the basis of the CO_2/N_2 ratio, three groups of interstitial soil gases were distinguished, as follows: (i) group *A*, characterized by a chemical composition largely dominated by CO_2, with CO_2/N_2 ratios higher than 10 and up to 27, (ii) group *B*, with CO_2/N_2 ratios ranging from 1.28 to 9.53, and (iii) group *C*, with a N_2-dominated composition and CO_2/N_2 ratios ≤0.62.

Group *A* soil gases were characterized by relevant concentrations of CO_2 (≥900 mmol/mol), H_2S (from 0.06 to 3.30 mmol/mol) and CH_4 (from 0.02 to 0.13 mmo/mol). Concentrations of N_2, O_2 and Ar ranged from 36 to 89 mmol/mol, from 0.51 to 12 mmol/mol and from 0.85 to 2.20 mmol/mol, respectively.

Similarly to *A* soil gases, those of group *B* were dominated by CO_2 (≤896 mmol/mol). On average, lower concentrations of H_2S and CH_4 relative to those measured in the *A* soil gases were detected (ranging from 0.06 to 2.10 mmol/mol and from 0.01 to 0.12 mmol/mol), whereas N_2, O_2 and Ar showed higher contents (from 94 to 395 mmol/mol, from 5.10 to 104 mmol/mol and from 2.30 to 9.90 mmol/mol, respectively).

Group *C* soil gases, showing N_2, O_2 and Ar concentrations ≥484, ≥136 and ≥ 11 mmol/mol, respectively, had CO_2 and CH_4 abundances of ≤302 and ≤ 0.03 mmol/mol, respectively, whereas H_2S was below the detection limit.

The total content of VOCs, ranging from 0.05 to 1.15 μmol/mol, increased with the CO_2/N_2 ratio, the highest and lowest concentrations being generally measured in the groups *A* (ΣVOCs ≥0.15 μmol/mol) and *C* (ΣVOCs ≤0.13 μmol/mol). The organic fraction was largely dominated by alkanes (ranging from 73 to 97% with respect to the ΣVOCs), mainly consisting of ethane (up to 0.61 μmol/mol) and propane (up to 0.15 μmol/mol), with minor amounts of iso-butane (up to 0.026 μmol/mol), normal-butane (up to 0.015 μmol/mol) and C_{5+} alkanes (up to 0.16 μmol/mol). The relative abundances of alkanes generally increased as the CO_2/N_2 ratio decreased, with values ranging from 82 to 91 %ΣVOCs, from 73 to 97 %ΣVOCs, and from 85 to 96 %ΣVOCs in groups *A*, *B* and *C*, respectively (Fig. 2). Moreover, S-bearing compounds were almost exclusively detected in the *A* soil gases (≤0.3 %ΣVOCs and up to 0.0012 μmol/mol), although they were occasionally measured in the *B* soil gases (≤0.2 %ΣVOCs and up to 0.0009 μmol/mol). Alkenes showed an opposite trend with respect to alkanes, with relative abundances up to 11.8 %ΣVOCs in *A* soil gases (i.e. ≤0.110 μmol/mol) and ≤8.7 %ΣVOCs (i.e. ≤0.011 μmol/mol) in *C* soil gases (Fig. 2). No clear trends were observed between the relative abundances of aromatic and cyclic compounds (ranging from 0.2 to 2.4 %ΣVOCs and from 0.5 to 2.5 %ΣVOCs, respectively) among the analyzed soil gases. The concentrations of aromatic and cyclic compounds in groups *A* and *B* (≤0.013 and ≤ 0.012 μmol/mol, respectively) were comparable, whereas those measured in *C* soil gases were lower (≤0.0015 and ≤ 0.0018 μmol/mol, respectively). Differently, O-bearing compounds, specifically aldehydes, ketones and carboxylic acids, were strongly enriched in *B* soil gases (up to 17 %ΣVOCs and 0.182 μmol/mol) with respect to those measured at both groups *A* and *C* (≤4.5 %ΣVOCs and up to 0.050 and 0.005 μmol/mol, respectively; Fig. 2).

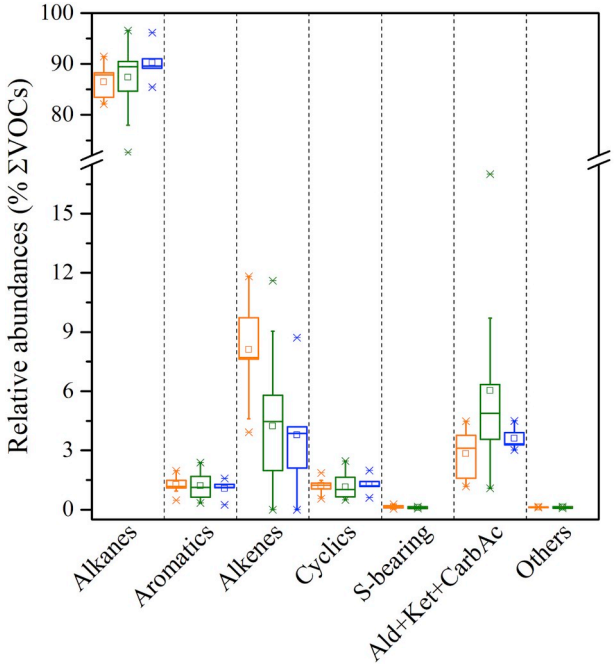

Fig. 2. Box plots of relative abundances (expressed as %ΣVOCs) of alkanes, aromatics, alkenes, cyclics, S-bearing compounds, aldehydes + ketones + carboxylic acids, and other VOCs in *A* (orange boxes), *B* (green boxes) and *C* (blue boxes) soil gases from Cava dei Selci. (For interpretation of the references to colour in this figure legend, the reader is referred to the Web version of this article.)

4.3. Soil fluxes

The soil CO_2, CH_4 and H_2S fluxes were measured at 81 sites in an area of about 1070 m^2 within the abandoned stone quarry. The ΦCO_2 values ranged from 13.7 to 13,638 g m^{-2} day^{-1}, whereas lower ΦCH_4 (up to 2.21 g m^{-2} day^{-1}) and ΦH_2S (up to 74.4 g m^{-2} day^{-1}) values were measured (Table 3).

As expected, relatively high ΦCO_2 (from 833 to 13,638 g m^{-2} day^{-1}), ΦCH_4 (up to 1.54 g m^{-2} day^{-1}) and ΦH_2S (up to 74.4 g m^{-2} day^{-1}) values (Table 3) were recorded in *A* soil gas sampling sites, whereas those from *C* sites were relatively low (≤344, ≤0.01 and ≤ 0.01 g m^{-2} day^{-1}, respectively; Table 3). Intermediate CO_2, CH_4 and H_2S soil fluxes (up to 3,669, 0.74 and 13.53 g m^{-2} day^{-1}) were measured in *B* soil gas sampling sites (Table 3).

In Fig. 3, the dot maps of soil CO_2, CH_4 and H_2S fluxes measured in the abandoned stone quarry are reported (Fig. 3a,c,d), together with the map of ΦCO_2 values produced by the sGs method (Fig. 3b). The highest emission zone was recognized in the SE portion of the study area, where the highest ΦCO_2, ΦCH_4 and ΦH_2S values were also measured by previous studies (e.g. Carapezza et al., 2003, 2012). This indicates that the anomalous degassing zone is well identified in space and time.

4.4. Measurements of air pollutants

4.4.1. Gas concentrations and $\delta^{13}C$-CO_2 values in air at the fixed measuring stations

The main statistical parameters of the CO_2, H_2S, SO_2 and GEM concentrations and $\delta^{13}C$-CO_2 values measured in F1 and F2 (Fig. 1c,e,f) in April 2016 are reported in Table 4.

At F1, CO_2 ranged from 874 to 1514 mg/m^3 on April 5 and from 896 to 2782 mg/m^3 on April 6. These values exceeded the typical CO_2 concentration in air suggesting that an external source of carbon dioxide contributed to the composition of air at F1 site. Throughout the time window of the survey, the H_2S concentrations ranged from 53 to

Table 3
Soil CO_2, CH_4 and H_2S fluxes (expressed in g m^{-2} day^{-1}) measured in the abandoned stone quarry of Cava dei Selci.

ID	ΦCO$_2$ (g m-2 day-1)	ΦCH$_4$ (g m-2 day-1)	ΦH$_2$S (g m-2 day-1)
1	122	0.01	
2	5125	0.74	14.19
3	3669	0.74	13.53
4	13638	1.54	20.45
5	12640	1.50	74.40
6	7734	0.94	44.64
7	1030	0.04	
8	14		0.01
9	5191	0.94	14.73
10	4373	0.79	12.28
11	1319	0.15	5.37
12	16		
13	833	0.10	4.56
14	8134	1.14	14.44
15	1257	0.19	1.91
16	895	0.13	
17	344		
18	956	0.13	3.05
19	83		
20	114		
21	159		
22	2022	0.29	
23	1939	0.32	0.22
24	1223	0.14	0.04
25	842	0.10	0.02
26	1425	0.11	
27	2109	0.09	0.02
28	541		
29	2011	0.33	
30	2012	0.25	0.59
31	1063	0.04	0.03
32	661		
33	194		
34	461		
35	550		0.01
36	113		
37	1122	0.06	
38	3270	0.21	
39	212	0.03	
40	2865	0.12	0.07
41	889	0.10	
42	17	0.00	
43	1100	0.11	
44	144	0.01	
45	237		0.01
46	484	0.01	
47	339	0.00	0.00
48	338	0.02	
49	191		
50	71	0.00	0.00
51	334		
52	198	0.00	0.01
53	1316	0.21	0.00
54	140	0.01	
55	484	0.07	0.07
56	471	0.03	0.03
57	58	0.01	0.09
58	691	0.10	0.17
59	206	0.03	
60	2183	0.55	0.34
61	82	0.01	0.58
62	203	0.03	0.67
63	299	0.03	0.54
64	278	0.03	0.62
65	603	0.09	0.88
66	312	0.07	1.25
67	616	0.09	3.21
68	1364	0.20	4.46
69	964	0.15	5.28
70	1135	0.19	5.25
71	3041	0.41	7.67
72	1769	0.27	9.30
73	4929	1.19	12.20
74	2394	0.38	12.81
75	2918	0.40	13.33
76	4577	0.98	17.76
77	4014	0.77	43.96
78	4665	0.87	21.57
79	4885	1.05	19.09
80	8010	2.09	23.82
81	9286	2.21	47.71

982 µg/m^3 and from 41 to 568 µg/m^3, respectively, whereas those of SO_2 were ≤33 µg/m^3. At F2, the CO_2, H_2S and SO_2 concentrations measured on April 6 (up to 4590 mg/m^3, 34,407 µg/m^3 and 408 µg/m^3, respectively) were even higher than those measured at F1. On the contrary, the highest concentrations of GEM were measured at F1 (up to 195 ng/m^3 on April 5), while at F2 they varied from 35 to 137 ng/m^3.

The isotopic composition of CO_2 at F1 varied from −6.49 to −1.39‰ vs. V-PDB and from −6.10–1.84‰ vs. V-PDB on April 5 and 6, respectively, and from −8.11 to 0.09‰ vs. V-PDB at F2. The carbon isotope composition indicates that CO_2 was enriched in ^{13}C with respect to the composition of uncontaminated air ($\delta^{13}C$-CO_2 = −8‰ vs. V-PDB). Both the less negative and positive values of $\delta^{13}C$-CO_2 in air agreed with the isotope composition of CO_2 emitted from F1 site, demonstrating that soil degassing governs both the concentration and the carbon isotope composition of air-CO_2 in the surroundings of F1 site. Furthermore, high concentrations of CO_2 in air and positive $\delta^{13}C$-CO_2 values were generally associated with low wind speed throughout the survey.

During the air measurements in F1, the wind speed was ≤1.3 m/s on April 5, whereas on April 6 wind was basically absent. At F2, the wind speed was up to 0.9 m/s.

4.4.2. Gas concentrations in air within the residential area of Cava dei Selci

The main statistical parameters of the air pollutants (i.e. CO_2, H_2S, SO_2, GEM, CO and CH_4) measured within the residential area of Cava dei Selci (Fig. 1c) are reported in Table 4. The concentrations of CO_2 ranged from 767 to 1174 mg/m^3, whereas those of H_2S varied from 2.9 to 351 µg/m^3. The concentrations of SO_2 and GEM ranged from 5.5 to 15 µg/m^3 and from 19 to 33 ng/m^3, respectively. Methane and CO contents were up to 1.7 and 0.77 mg/m^3, respectively. Prevailing winds (from 0 to 0.9 m/s) blew from NNE, i.e. from the main emitting areas (Fig. 1c).

Air measurements were also performed inside a windowless private garage and in the aerated underground garage of a house (Fig. 1c; Table 4). While the GEM concentrations in the two garages were similar (~25 ng/m^3), those of CO_2, CO and SO_2 in the windowless garage were about 2 or 3 times higher than those recorded in the aerated basement. Methane concentrations in the windowless garage were up to 8 times higher (up to 11 mg/m^3; Table 4) than those measured in the aerated basement. Remarkably, H_2S in the windowless garage was up to 1358 µg/m^3, i.e. more than 100 times higher than that measured in the aerated basement (up to 9.2 µg/m^3).

5. Discussion

5.1. Origin of the endogenous gases

The CO_2-dominated gases emitted from Cava dei Selci were characterized by $\delta^{13}C$-CO_2 values (from 0.73 to 1.08‰ vs. V-PDB) comparable to those reported by Minissale et al. (1997) for gas manifestations from north-central Italy. These values, significantly higher than those expected for a shallow organic derivation for CO_2 (typically characterized by $\delta^{13}C$-CO_2 < -20‰ vs. V-PDB; Degens, 1969; Rollinson, 1993; Sano and Marty, 1995), were interpreted as related to

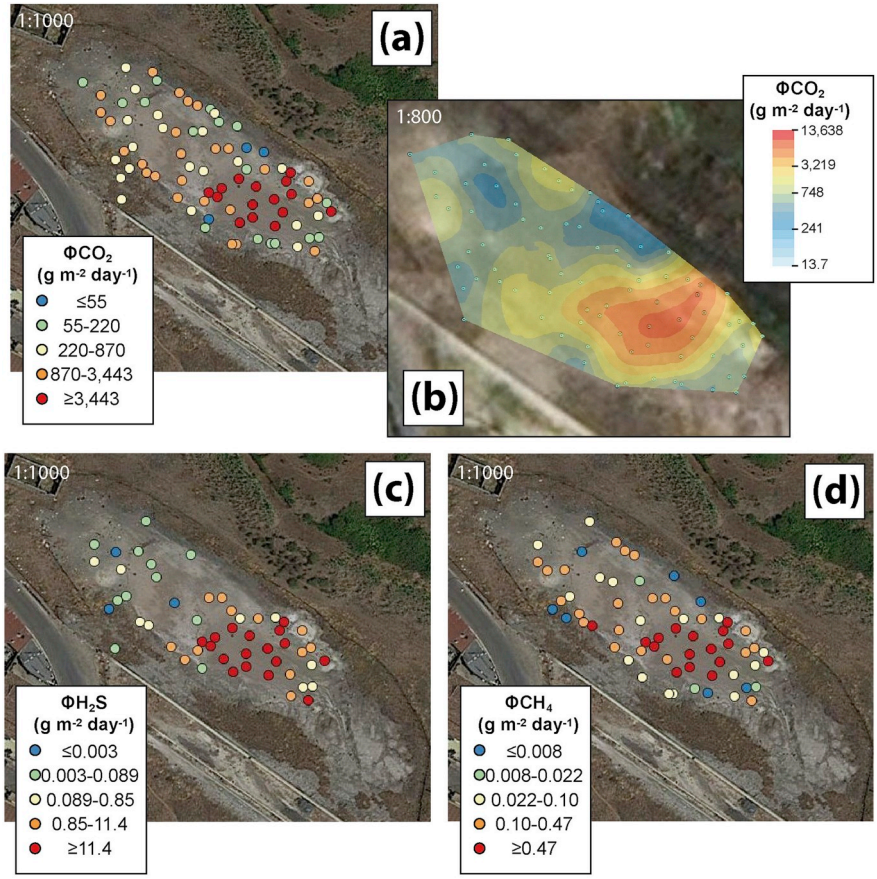

Fig. 3. Dot maps of soil (a) CO_2, (c) H_2S and (d) CH_4 fluxes measured in the abandoned stone quarry of Cava dei Selci. (b) The map of ΦCO_2 values produced by sGs method is also reported.

a deep high-temperature source (e.g. Giggenbach et al., 1988; Capasso et al., 1997; Chiodini and Frondini, 2001; Annunziatellis et al., 2003). According to Chiodini et al. (2004), in the peri-Tyrrhenian sector of central Italy (i.e. from the Larderello geothermal field in Tuscany to the Colli Albani volcanic complex in Latium), a large portion of CO_2 degassing at the surface or dissolved in ground waters originates from a deep mantle-related source, which would account for a total CO_2 release of 1.4×10^{11} mol/y. Gases from Cava dei Selci were also characterized by a significant amount of mantle He, as indicated by the relatively high R_c/R_a values (1.41) that were higher than those measured in gases emitted from the other Latium volcanic districts (i.e. from 0.2 to 0.6; Hooker et al., 1985). Similar R_c/R_a values (from 0.44 to 1.73) were measured in fluid inclusions of phenocrysts from the Colli Albani volcanic rocks (Martelli et al., 2004; Carapezza et al., 2012). Besides the deep source, metamorphic decarbonation processes also contribute to the CO_2 discharged at the surface in the Colli Albani area. Giggenbach et al. (1988) ascribed the relatively high $\delta^{13}C$-CO_2 values measured in gas discharges in the Colli Albani area to the involvement of marine carbonates in the production of CO_2. Carbonate assimilation in the upper crust is likely representing an important additional mechanism of CO_2 production in active volcanic zones from central-southern Italy (Iacono Marziano et al., 2007). In the $CO_2/^3He$ ratios vs. $\delta^{13}C$-CO_2 diagram (Fig. 4a), the Cava dei Selci gases plot along a mixing curve between the mantle and limestone end-members, confirming the twofold source. As shown in the Ar-N_2-He ternary diagram (Fig. 4b), N_2 from the Cava dei Selci gases is sourced by air and a deep N_2-rich source. Accordingly, the measured N_2/Ar ratios (up to 134) were higher than those of both air saturated water (ASW, 38) and air (83), confirming the presence of an excess, non-atmospheric N_2 (N_{2exc}). The amount of N_{2exc} can be estimated, as follows:

$$N_{2exc} = N_2 - [(N_2/Ar)_{atm} \times Ar] \quad (3)$$

where the $(N_2/Ar)_{atm}$ is the N_2/Ar ratio in either ASW or air, assuming that Ar is entirely derived from an atmospheric component. The validity of this assumption was confirmed by the measured $^{40}Ar/^{36}Ar$ and $^{38}Ar/^{36}Ar$ ratios, which were comparable to those of air (i.e. 296 and 0.188, respectively; Ozima and Podosek, 2002). The $N_{2exc}/^3He$ ratios ranged from 4.85×10^8 to 1.46×10^9, i.e. higher than that expected for a pure mantle contribution ($N_{2exc}/^3He$ ratio of 2.3×10^8; Marty and Zimmermann, 1999; Hilton et al., 2002; Taran, 2011), indicating an extra-atmospheric crustal source. According to Minissale et al. (1997), the N_2 excess observed in several gas manifestations from north-central Italy is likely derived from organic nitrogen and ammonium-rich feldspar and micas within the Paleozoic metasedimentary basement rocks. However, the relatively low CH_4 contents measured in this study allow to exclude the occurrence of a significant organic nitrogen source, as also reported by previous investigations (Annunziatellis et al., 2003; Carapezza et al., 2003; Carapezza and Tarchini, 2007).

As far as the origin of CH_4 is concerned, the $\delta^{13}C$-CH_4 values measured in gas manifestations from Cava dei Selci were higher than those expected for microbially-produced CH_4 ($\leq$-50‰ vs. V-PDB) and thermogenic CH_4 (from −50 to −30‰ vs. V-PDB) (Whiticar, 1999; McCollom and Seewald, 2007). Moreover, the $CH_4/(C_2H_6 + C_3H_8)$ ratio (the so-called "Bernard parameter", after Bernard et al., 1978) varied from 214 to 231, i.e. intermediate between values characterizing gases from thermogenic (< 100) and microbial sources (> 1000). Hence, the chemical and isotopic features of CH_4 and light alkanes are not consistent with a classical interpretation. In Fig. 4c, the gas manifestations from Cava dei Selci approach the compositional field ($\delta^{13}C$-CH_4 from −24 to −13‰ vs. V-PDB; $CH_4/(C_2H_6 + C_3H_8) > 1000$) considered by some authors (e.g. McCollom and Seewald, 2007) typical of a purely

Table 4
Summary statistics (minimum, maximum, average and standard deviation) of atmospheric concentrations of CO_2, H_2S, SO_2, GEM, CO and CH_4 and $\delta^{13}C$-CO_2 values recorded by the fixed measuring stations (F1 and F2), in the residential area of Cava dei Selci and inside two private garages.

	Date	Time Interval	CO2 (mg/m3)				H2S (μg/m3)				SO2 (μg/m3)			
			min	max	average	st.dev.	min	max	average	st.dev.	min	max	average	st.dev.
F1	April 5, 2016	14:51–18:01	874	1514	1086	133	53	982	213	156	11	24	17	2.7
F1	April 6, 2016	10:52–12:10	896	2782	1078	235	41	568	147	111	15	33	22	4.2
F2	April 6, 2016	16:36–17:32	809	4590	2825	1211	179	34,407	22,238	9974	26	408	225	105
Residential area	April 7, 2016	09:34–11:23	767	1174	807	64	2.9	351	43	67	5.5	15	9.9	2.1
Aerated garage	April 7, 2016	09:44–09:49	792	916	864	46	7.6	9.2	8.4	0.63	6.6	10	8.4	1.3
Windowless garage	April 7, 2016	10:11–10:15	1776	2010	1861	80	1095	1358	1215	87	22	24	23	0.87

	GEM (ng/m3)				δ13C-CO2 (‰ vs. V-PDB)				CH4 (mg/m3)				CO (mg/m3)			
	min	max	average	st.dev.	min	max	average	st.dev.	min	max	average	st.dev.	min	max	average	st.dev.
F1	47	195	101	31	−6.49	−1.39	−3.61	0.98	n.a.	n.a.	n.a.	n.a.	n.a.	n.a.	n.a.	n.a.
F1	22	125	52	24	−6.10	1.84	−2.86	1.54	n.a.	n.a.	n.a.	n.a.	n.a.	n.a.	n.a.	n.a.
F2	35	137	77	22	−8.11	0.09	−2.47	2.10	n.a.	n.a.	n.a.	n.a.	n.a.	n.a.	n.a.	n.a.
Residential area	19	33	25	3.7	n.a.	n.a.	n.a.	n.a.	1.3	1.7	1.4	0.05	0.46	0.77	0.60	0.10
Aerated garage	22	26	24	1.4	n.a.	n.a.	n.a.	n.a.	1.3	1.3	1.3	0.001	0.50	0.73	0.59	0.11
Windowless garage	25	28	27	1.2	n.a.	n.a.	n.a.	n.a.	10	11	11	0.29	0.56	1.6	1.2	0.48

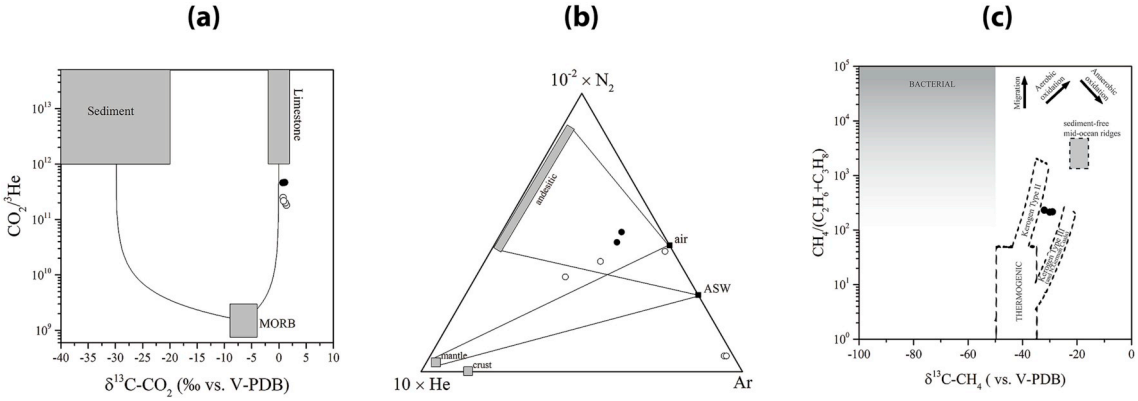

Fig. 4. (a) $CO_2/^3He$ vs. $\delta^{13}C\text{-}CO_2$ binary diagram (after Sano and Marty, 1995) for punctual gas emissions from Cava dei Selci (black circles = data from this study; white circles = data from Carapezza and Tarchini, 2007; Carapezza et al., 2012). Mid-ocean ridge basalt (MORB), limestone and sediment fields are also indicated. (b) Ar-N_2-He ternary diagram (after Giggenbach et al., 1983; Giggenbach, 1991, 1996) for gases discharged from Cava dei Selci (black circles = data from this study; white circles = data from Giggenbach et al., 1988; Chiodini and Frondini, 2001; Carapezza et al., 2012). Andesitic, mantle and crustal end-members are also reported, together with those of air and air saturated water (ASW). (c) $CH_4/(C_2H_6+C_3H_8)$ vs. $\delta^{13}C\text{-}CH_4$ binary diagram for punctual gas emissions from Cava dei Selci (after Bernard et al., 1978; Whiticar, 1999). Existence fields of biogenic origin (microbial and thermogenic) and unsedimented mid-oceanic ridges, sediment-covered ridges and igneous rocks are reported (McCollom and Seewald, 2007, and references therein) for comparison. The black arrows depict the trends related to migration, aerobic oxidation and anaerobic oxidation (e.g. Moore et al., 2018).

abiogenic origin. Tassi et al. (2012) also reported similar values for CO_2-rich gas manifestations from the whole peri-Tyrrhenian part of central Italy (Tuscany and Latium) and ascribed to the addition of thermogenic gases due to secondary CH_4 production from CO_2 reduction. Nevertheless, the shift towards higher $CH_4/(C_2H_6+C_3H_8)$ ratios and $\delta^{13}C\text{-}CH_4$ of the gas samples from Cava dei Selci with respect to the typical thermogenic field, as observed in Fig. 4c, could be similarly ascribed to either a migrated hydrocarbon-rich fluid that experienced oxidation approaching the surface or a highly-oxidized, hydrocarbon-rich fluid (Harkness et al., 2017; Moore et al., 2018), without the involvement of abiotic fluids. The occurrence of a thermogenic organic gas source at Cava dei Selci was confirmed by the presence of C_{4+} alkanes, benzene and other aromatics. Similarly, other gas species, such as H_2S and GEM, were likely produced as a result of gas reactions, re-equilibrations and mobilization processes in the hydrothermal reservoir (Minissale et al., 1997; Bagnato et al., 2009). In particular, the origin of H_2S can be ascribed to thermogenic reduction of Triassic anhydrites, which are present at the base of the Mesozoic carbonate sequence (Giordano et al., 2014), as also observed in H_2S-bearing gases discharging from the northern part of the Roman Magmatic Province (e.g. Sabatini and Vicano-Cimino volcanic districts; Cinti et al., 2011, 2014, 2017). In particular, the H_2S production from the evaporitic formations may proceed through thermochemical sulfate reduction (TSR), a process involving hydrocarbons, according to the following reaction (Worden and Smalley, 1996):

$$\text{anhydrite} + \text{hydrocarbons} \rightarrow \text{calcite} + H_2S + H_2O \pm S \pm CO_2 \quad (4)$$

and primarily CH_4, as follows (Worden and Smalley, 1996):

$$CaSO_4 + CH_4 \rightarrow CaCO_3 + H_2S + H_2O \quad (5)$$

5.2. Estimation of gas output through diffuse degassing

In order to estimate the total output of CO_2, CH_4 and H_2S from the study area, the population partitioning method proposed by Sinclair (1974) was applied. The probability plots of $\ln\Phi_{CO2}$, $\ln\Phi_{CH4}$ and $\ln\Phi_{H2S}$ are reported in Fig. 5. As suggested by Fig. 5a, most $\ln\Phi_{CO2}$ variations can be ascribed to a single population, with the exception of (i) some values with low ΦCO_2 values ($\leq 17\ g\ m^{-2}\ day^{-1}$), likely representing biological CO_2 from soil respiration and (ii) some outliers with ΦCO_2 $\geq 7734\ g\ m^{-2}\ day^{-1}$, likely related to the occurrence of fractures causing an increase of soil permeability at a local scale. Differently from $\ln\Phi_{CO2}$, the probability plots of $\ln\Phi_{CH4}$ (Fig. 5b) and $\ln\Phi_{H2S}$ (Fig. 5c) suggest the presence of two different populations (A and B). This cannot be related to the soil permeability, as this parameter should likewise affect ΦCO_2 producing an analogous polymodal distribution of $\ln\Phi_{CO2}$. Hence, the populations recognized in Fig. 5b and c are likely reflecting the occurrence of physicochemical processes affecting CH_4 and H_2S with no influence on CO_2. The total output of CO_2 and H_2S from the study area was estimated in 2660 and 12 kg day^{-1}, whereas the total emission of CH_4 resulted in 0.42 kg day^{-1}.

5.3. Processes affecting gases emitted through diffuse degassing

The soil gases emitted from the study area showed anomalously high concentrations of components not originated by an atmospheric source. The soil gas concentrations of CH_4 and H_2S displayed a moderate correlation with the ΦCH_4 and ΦH_2S values measured at the same points, whereas a better correspondence was observed between CO_2 contents and ΦCO_2 values (Fig. 6).

Although the CO_2 concentration in the soil is generally depending on biotic processes (e.g. microbial activity) and environmental factors (e.g. soil temperature and moisture content, soil permeability), the positive correlation with the ΦCO_2 values suggests that the fate of this gas in the abandoned quarry was strictly controlled by the supply of fluids from the deep reservoir. Accordingly, the CO_2 concentrations in interstitial soil gases were inversely correlated with those of atmospheric gases (N_2, O_2 and Ar).

However, as shown in the CO_2-H_2S-N_2 ternary diagram (Fig. 7a), the CO_2/H_2S ratios were largely variable, ranging from 283 to 16,143, i.e. 2–3 orders of magnitude higher than those measured at the punctual gas emissions (from 89 to 177). It is worthwhile to mention that, during the geochemical survey at the Cava dei Selci emitting area, the water table was found at around 40 cm depth or shallower, which emerges above the ground during the rainy season forming a stagnant water pool, strongly interacting with the percolating gases (Giggenbach et al., 1988). The N_2/Ar ratio in the interstitial soil gases varies in a narrow range (from 34 to 50), which is similar to that of ASW, suggesting that the primary deep fluids are partly modified before reaching the surface. In addition, as the deep-seated gases percolate through shallow ground waters, H_2S is oxidized, as follows:

$$H_2S_{(g)} + 2O_{2(aq)} = 2H^+_{(aq)} + SO_4^{2-}{}_{(aq)} \quad (6)$$

Accordingly, the composition of the seasonal stagnant pool water

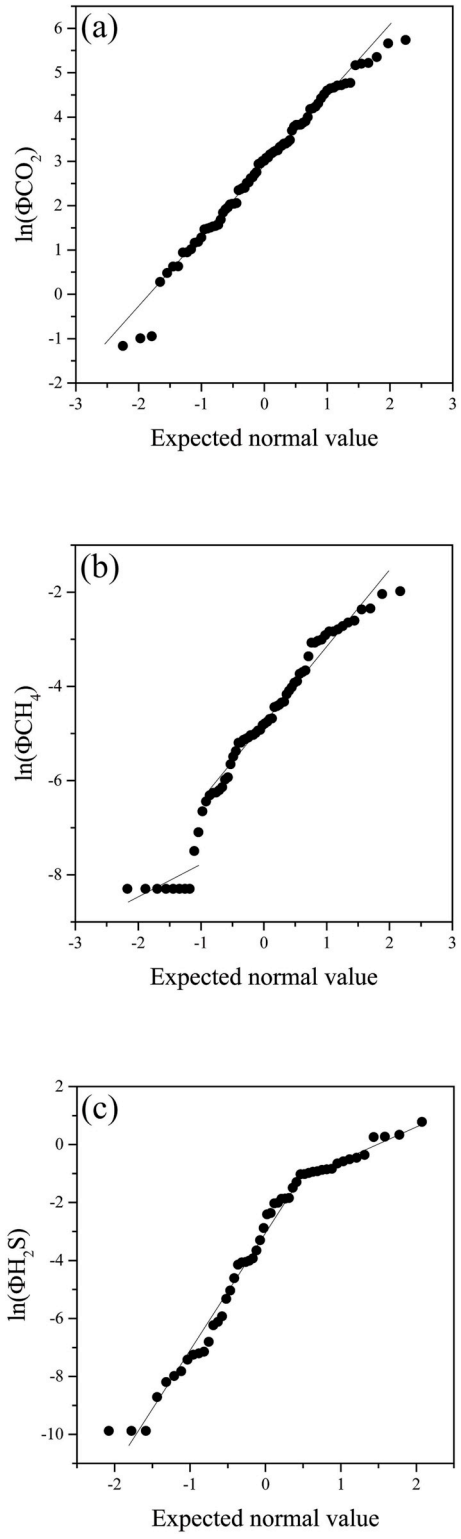

Fig. 5. Probability plots of (a) $\ln\Phi_{CO2}$, (b) $\ln\Phi_{CH4}$ and (c) $\ln\Phi_{H2S}$.

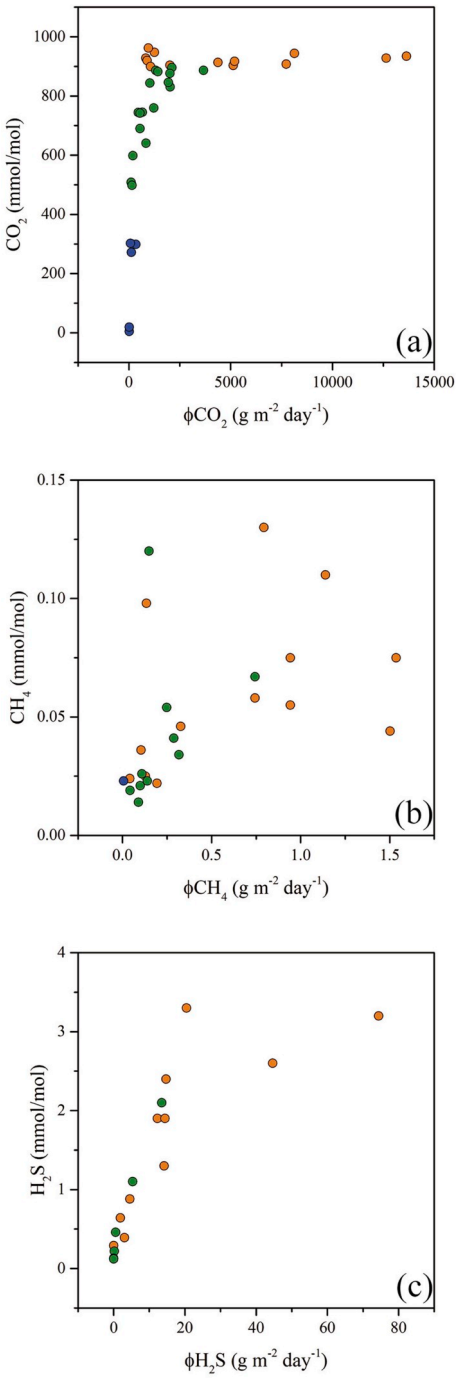

Fig. 6. (a) CO_2 vs. ΦCO_2, (b) CH_4 vs. ΦCH_4 and (c) H_2S vs. Φ H_2S binary diagrams (*A* soil gases: orange circles; *B* soil gases: green circles; *C* soil gases: blue circles). (For interpretation of the references to colour in this figure legend, the reader is referred to the Web version of this article.)

occurring in the abandoned stone quarry is characterized by a SO_4–dominated composition (Giggenbach et al., 1988). Then, the two trends depicted in Fig. 7a are related to (i) oxidation, and (ii) air dilution processes. A similar distribution is observed in Fig. 7b where H_2S is replaced by CH_4. Methane has a low solubility in water and consequently it is not expected to be scrubbed when interacting with shallow ground waters. On the other hand, methanotrophic bacteria may catalyze the oxidation of CH_4 to methanol and, eventually, CO_2 (e.g. Rojo, 2009). Microbially-driven oxidative processes at shallow depths are generally enhanced as the diffuse degassing decreases, determining an enrichment in O-bearing organic compounds in soil gases with respect to punctual gas emissions (e.g. Tassi et al., 2015a,b and references therein). Nevertheless, *A* soil gases were depleted in O-bearing organic compounds relative to the gas vents and a decrease in the relative abundances of these compounds was observed in *C* with respect to *B* soil gases (Fig. 2). It has to be considered that O-bearing VOCs, such as the intermediates of CH_4 oxidation to CO_2, are water soluble due to the polarity of their molecules. Thus, they can be affected by the interaction with the shallow water table. Similarly, the decrease in the alkenes at

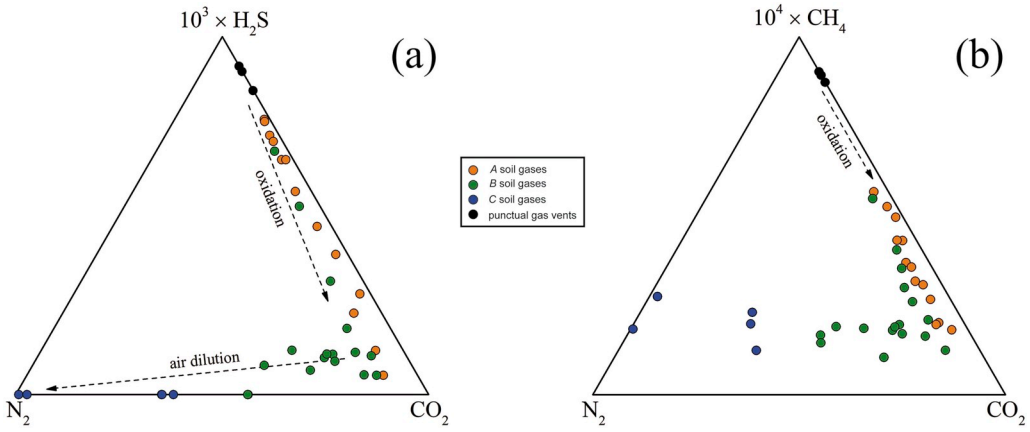

Fig. 7. (a) CO_2-H_2S-N_2 and (b) CO_2-CH_4-N_2 ternary diagrams for interstitial soil gases (*A* soil gases: orange circles; *B* soil gases: green circles; *C* soil gases: blue circles) and punctual gas emissions (black circles). (For interpretation of the references to colour in this figure legend, the reader is referred to the Web version of this article.)

decreasing CO_2/N_2 ratios in the soil gases (Fig. 2) is likely related to the high reactivity of the C=C bond that makes these compounds prone to degradation processes in an aquatic environment, e.g. hydration. Selective gas dissolution could also explain the enrichment in apolar-saturated hydrocarbons (i.e. alkanes) recorded in the soil gases with respect to those occurring at the gas vents.

Accordingly, the chemical composition of interstitial soil gases is expected to be controlled by both (i) structural and lithological factors (e.g. brittle structures and permeability), which govern the flux of deep hydrothermal fluids, and (ii) chemical rearrangements, induced by gas-water interaction processes, microbial activity and increasingly oxidizing conditions at shallow depths. Among the endogenous gases, reduced and highly soluble species are expected to be particularly affected by secondary processes during the upward motion of fluids from the deep reservoir up to the surface. This implies that substantial compositional changes occur when gases from punctual vents and interstitial soils are compared.

5.4. Impact on air quality

5.4.1. Fixed measuring stations

The presence of favorable conditions to the emissions of CO_2- and H_2S-rich gases from the study area poses severe risks to the health of local population (e.g. Annunziatellis et al., 2003; Beaubien et al., 2003; Carapezza et al., 2003, 2010, 2012). The CO_2 concentrations in air measured at F1 and F2 stations (~1080 and 2825 mg/m^3 on average, respectively) were significantly higher than the global monthly average concentration of atmospheric CO_2, i.e. 733 mg/m^3 (Scripps CO_2 Program). However, the highest value (4590 mg/m^3) measured at F2 exceeded neither the 8 h time weighted average (TWA) threshold of 9000 mg/m^3 (NIOSH, 1996; Department of Health and Human Services - NIOSH, 2007) nor the 15 min short-term exposure limit (STEL) of 54,000 mg/m^3 (NIOSH, 1996; Department of Health and Human Services - NIOSH, 2007). Nevertheless, a recent study by Martrette et al. (2017) demonstrated that prolonged exposure to relatively low CO_2 doses (1260 mg/m^3 for 6 h a day for 15 days) can cause behavioral and physiological changes in mammals, affecting general behavior, hormonal status and myosin heavy chain (MHC) profile of diaphragm and oral respiratory muscles of young female rats. Noteworthy, CO_2 concentrations > 1260 mg/m^3 were occasional at F1 and frequent at F2.

In Fig. 8, the δ^{13}C-CO_2 values are plotted against the ratios between the concentration of CO_2 in unpolluted air (733 mg/m^3) and the concentrations of CO_2 measured at F1 and F2. The data from F2 seem to describe a mixing curve between air (δ^{13}C-CO_2 = −8‰ vs. V-PDB; Scripps CO_2 Program) and the endogenous CO_2 source whose δ^{13}C-CO_2 value result in the range of 0.73–1.39‰ vs. V-PDB, in agreement with those measured in gases from punctual vents (Giggenbach et al., 1988;

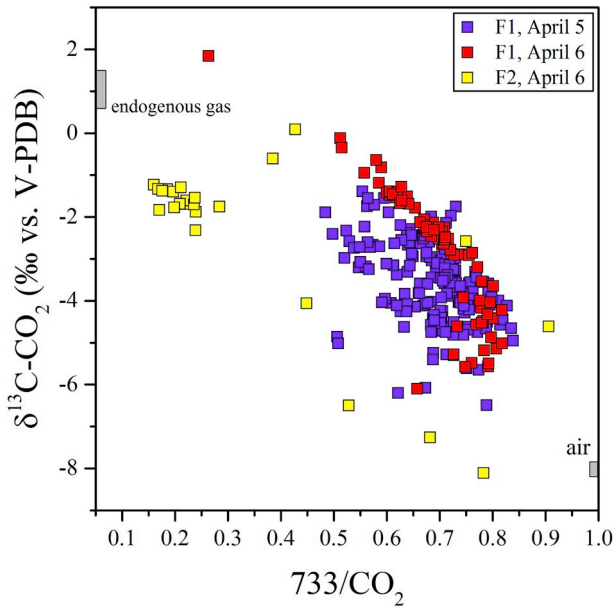

Fig. 8. δ^{13}C-CO_2 vs. 733/CO_2 binary diagram of air measurements in F1 on April 5 (violet squares) and 6 (red squares) and in F2 (yellow squares). Air and endogenous gas (grey fields) are plotted for comparison. (For interpretation of the references to colour in this figure legend, the reader is referred to the Web version of this article.)

Annunziatellis et al., 2003; Carapezza and Tarchini, 2007; Carapezza et al., 2012; this study). While endogenous gas was adjectively discharged at F2 through the blowing well, diffusive transport process exerted a pivotal influence on the total output of endogenous gas at F1. Accordingly, the δ^{13}C-CO_2 values measured at F1, which are slightly higher than those measured at F2 and those expected for a simple mixing between air and endogenous gas, were likely due to isotopic fractionation processes occurring in the soil layers in response to gas diffusion and microbial activity (Cerling et al., 1991; Capasso et al., 2001; Camarda et al., 2007; Federico et al., 2010; Tassi et al., 2015b).

H_2S measured in air at the fixed measuring stations (≥41 μg/m^3) largely exceeded the 30-min average concentration considered as the threshold for odor annoyance in ambient air (7 μg/m^3; WHO, 2000). The average (213 μg/m^3) and maximum (568 μg/m^3) H_2S air concentrations measured at F1 on April 5 and 6, 2016, respectively, were significantly higher than the air quality guideline threshold (150 μg/m^3; WHO, 2000). At F2, this limit was overcome during the whole measurement period as the H_2S concentrations varied from 179 to

22,238 μg/m^3, i.e. in some cases higher than the NIOSH recommended exposure limit (REL) in workplaces (15,000 μg/m^3; Department of Health and Human Services (NIOSH), 2007). These concentrations were largely lower than those measured by Carapezza et al. (2010, 2012) from 0 to 7 a.m. (up to 708 mg/m^3 at 20 cm above the ground). This confirms that the risk of exposure to hazardous gas concentrations drastically increases during the night, when lack of wind and sun irradiation favor gas accumulation at ground level (e.g. Tassi et al., 2009; Vaselli et al., 2011). At Cava dei Selci, the persistence of H_2S in air with concentrations higher than the TWA threshold in the diurnal period suggests that H_2S, rather than CO_2, represents the main threat for inhabitants. The CO_2/H_2S ratios in air (from 1016 to 28,139 and from 24 to 4235 at F1 and F2, respectively) were higher than those measured in the gas vents (from 89 to 177), likely due to the contribution from diffuse degassing from the soil where H_2S is partially consumed by oxidation processes (at F1) and dissolution in the aquifer (at F2). Further H_2S consumption likely occurred in air. Whilst CO_2 can be considered chemically inert at ambient conditions, H_2S can undergo oxidation to SO_2 by reacting with ozone (O_3), molecular oxygen (O_2) or hydroxyl radicals ($HO^{\bullet}$). Since H_2S oxidation involving O_3 and O_2 is slow under atmospheric conditions, the formation of SO_2 from H_2S in air is mainly proceeding through reaction with $HO^{\bullet}$ via production of $HS^{\bullet}$ radical, as follows:

$$H_2S + HO^{\bullet} = HS^{\bullet} + H_2O \quad (7)$$

$$HS^{\bullet} + O_2 = HO^{\bullet} + SO^{\bullet} \quad (8)$$

$$SO^{\bullet} + O_2 = SO_2 + O^{\bullet} \quad (9)$$

It is worth noting that the average SO_2 air concentrations exceeded the WHO guideline value of 20 μg/m^3 (as 24-h average; WHO, 2006) at both F1 and F2 on the 6th of April, where the highest SO_2 air concentration approached the 10 min average threshold of 500 μg/m^3 recommended by WHO (2000, 2006), although SO_2 was below the detection limit in gases from the punctual vents.

These results show that secondary pollutants, i.e. those produced after the input of gases in air from a contaminant source, may have a strong impact on air quality. Sulfur dioxide is a strong-irritant gas (e.g. Petruzzi et al., 1994; Tunnicliffe et al., 2001), causing inflammation of eyes, nose and throat at 13–26 mg/m^3 and leading to respiratory failure at 79–105 mg/m^3 (WHO, 2006). Moreover, it affects trees and plants by damaging foliage and decreasing growth and contributes to acid rain, harming ecosystems and damaging materials and buildings (WHO, 2000).

5.4.2. Mobile multi-instrumental station

As the prevailing winds blew from NNE, gases emitted from the abandoned stone quarry and the gas-blowing well moved towards the nearby residential area (Fig. 9). Accordingly, anomalous CO_2 and H_2S concentrations ($\geq$767 mg/m^3 and $\geq$2.9 μg/m^3, respectively) were detected along the measurement pathway, especially in the sector facing the abandoned quarry where CO_2 and H_2S were up to 914 mg/m^3 and 225 μg/m^3, respectively (Fig. 9a,e). The concentrations of H_2S were higher than the odor annoyance threshold in a large portion of the residential area and up to distances > 250 m from the abandoned stone quarry (Fig. 9e). Despite the common source of these two gases, large variations of the CO_2/H_2S ratios in air (from 2592 to 203,319; Fig. 9b) were observed. Since the concentrations of the inert CO_2 in air are mainly controlled by dilution during its transport from the source, the remarkable changes observed in the CO_2/H_2S ratios are to be ascribed to either (i) chemical processes affecting and consuming H_2S, i.e. chemical oxidation to SO_2, or (ii) different transport dynamics of the two gases in air. Whilst the CO_2/H_2S ratios increased with the distance from the emitting area (Fig. 9b), the H_2S/SO_2 ratios decreased (Fig. 9g), supporting the hypothesis of a progressive oxidation of H_2S. Nevertheless, SO_2 concentrations measured in the residential area ($\leq$15 μg/m^3; Fig. 9f) were lower than the limit (20 μg/m^3) for ambient air reported by WHO (2006). A relatively high H_2S/SO_2 ratio (53; Fig. 9g) was measured in correspondence with the highest CO_2 and H_2S concentrations (1174 mg/m^3 and 351 μg/m^3, respectively; Fig. 9a,e). Surprisingly, this site was located in front of the descending vehicular access to a private garage (Fig. 1c), quite far from the main emitting zone. To verify the cause(s) of this anomaly, the mobile multi-instrumental station was positioned inside private garages to carry out indoor measurements that revealed alarmingly high pollutants concentrations (CO_2 concentrations up to 2010 mg/m^3, H_2S and SO_2 concentrations exceeding the 24-h average thresholds, i.e. up to 1358 and 24.5 μg/m^3, respectively). This demonstrated how the hazard related to endogenous gas emission may dramatically increase under poorly ventilated conditions, especially at basement and ground levels. It is worth noting that, at about 150 m ESE from this point, H_2S was detected at high concentration (225 μg/m^3) in front of a house that was evacuated in March 2018 due to severe odor nuisance. The installation of an early warning alarm system to continuously monitor at least CO_2 and H_2S is highly recommended to avoid serious health problems to the inhabitants of these houses.

Other pollutants potentially affecting the air quality at Cava dei Selci included GEM, CO and CH_4. The GEM concentrations in air at F1 and F2 (up to 195 and 137 ng/m^3, respectively) were significantly higher than the typical background concentration in unpolluted areas, i.e. ~2 ng/m^3 (USEPA, 1997; Ebinghaus et al., 2002). Along the measuring pathway in the residential area GEM ranged from 19 to 33 ng/m^3, i.e. above the mean concentrations measured in some urban environments (Denis et al., 2006 and references therein). However, the GEM spatial distribution was decoupled with respect to those of CO_2 and H_2S (as confirmed by the CO_2/GEM dot map; Fig. 9i), since it increased moving from NNE to SSW, the highest values being measured > 250 m away from the emitting area (Fig. 9h). This suggests a different transport dynamic of GEM with respect to those of CO_2 and H_2S, controlled by peculiar processes regulating the behavior of the pollutant once released in the air. GEM is in fact relatively stable in the atmosphere (e.g. Schroeder and Munthe, 1998; Sommar et al., 2001; Fitzgerald and Lamborg, 2007). It has a low solubility in water and little tendency to be scavenged by physical removal processes, e.g. dry deposition on vegetation (Fu et al., 2010). Moreover, meteorological parameters such as temperature, humidity and wind speed and direction were proven to exert a greater impact on GEM concentrations than photochemical reactions (e.g. Esbrí et al., 2016), contrarily to H_2S, which is more affected by secondary (oxidation) processes in air.

The concentrations of CO and CH_4 (from 0.46 to 0.77 mg/m^3 and from 1.3 to 1.7 mg/m^3, respectively) were largely higher than global background concentrations ($\leq$0.14 mg/m^3 and ~1.18 mg/m^3; WHO, 2000). The dot map of the CO_2/CH_4 ratios (Fig. 9c) closely resembles that of CO_2 levels (Fig. 9a), pointing to a negligible spatial variation of the CH_4 concentrations in air. Moreover, the CH_4 concentrations in air were comparable to those measured in other urban areas (~1.4 mg/m^3; e.g. Thi Nguyen et al., 2010), suggesting that its impact in the residential area is negligible. The distribution map of the CO_2/CO ratios (Fig. 9d) evidences higher values in the central portion of the residential zone and a faster decrease of CO concentrations in air with respect to those of CO_2 as the distance from the emitting source increased, suggesting that CO likely undergoes oxidation processes once it is released in air. Conversely, the decrease of the CO_2/CO ratios in distal areas from the emitting sources can likely be attributed to the influence of a different contaminant source, such as vehicular traffic. Consequently, the impact of CO due to the gas emissions is limited to the surroundings of the abandoned quarry, although the levels of CO in air, even inside the non-ventilated private garage, were largely lower than those measured in urban traffic environments (8-h average CO concentrations generally lower than 20 mg/m^3; WHO, 2000). Differently, CH_4 inside the windowless garage reached contents up to 11 mg/m^3, i.e. up to one order of magnitude higher than those recorded in outdoor ambient air, confirming the strong impact of the endogenous gases on

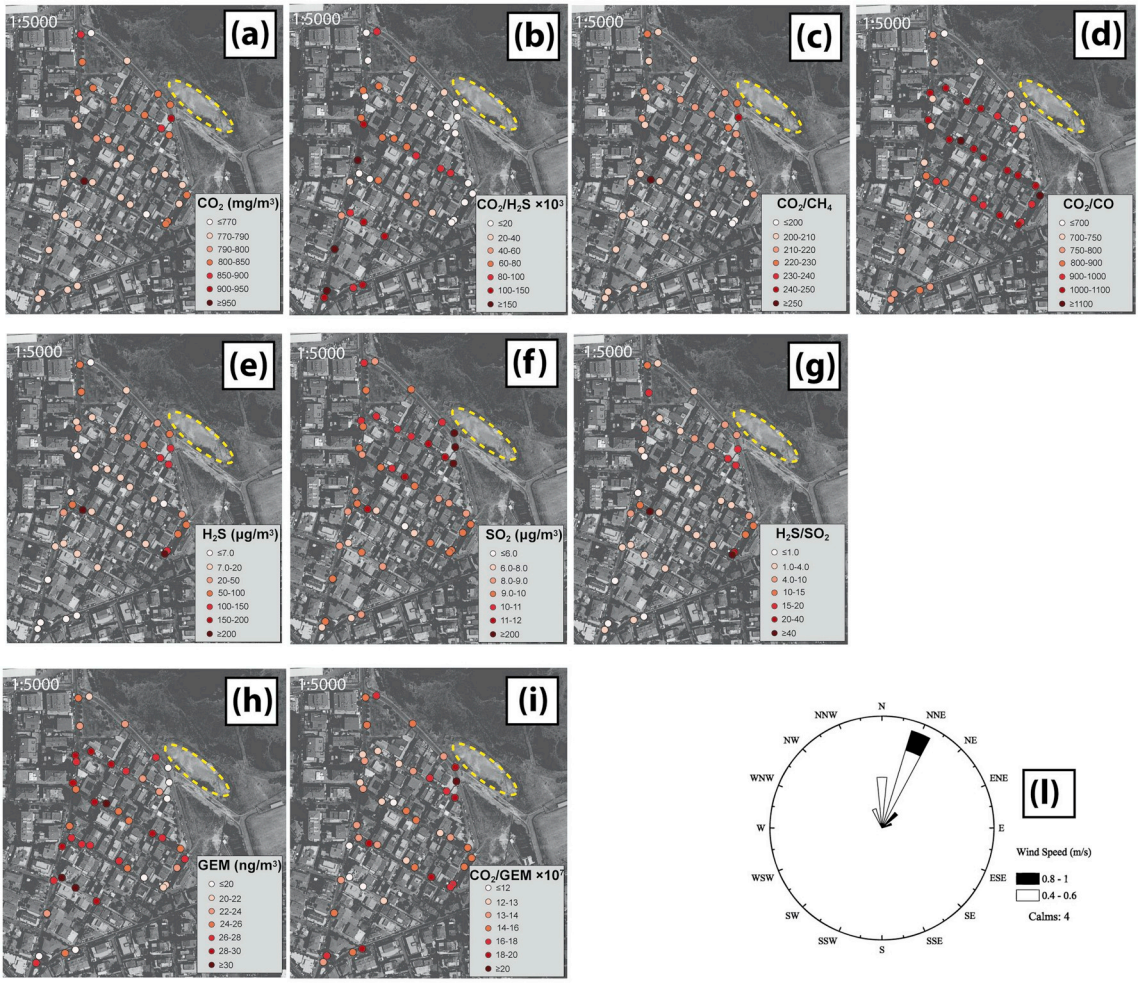

Fig. 9. Dot maps of air concentrations of (a) CO_2, (e) H_2S, (f) SO_2, (h) GEM and concentration ratios of (b) CO_2/H_2S, (c) CO_2/CH_4, (d) CO_2/CO, (g) H_2S/SO_2 and (i) CO_2/GEM measured in the residential area in Cava dei Selci. The yellow dashed ellipse identifies the location of the abandoned quarry. (l) Wind direction and speed. (For interpretation of the references to colour in this figure legend, the reader is referred to the Web version of this article.)

indoor environments.

6. Conclusions

Natural gas emissions and diffuse soil degassing strongly affect the air quality in the intensely urbanized area of Cava dei Selci (20 km SE of Rome) as testified by the lethal accidents that occurred in the past and caused by gas inhalation. The multi-parametric geochemical survey carried out in this area in April 2016 evidenced that CO_2, mainly originated by mantle and/or magmatic degassing with a minor crustal contribution, was the main constituent of the discharged gases, followed by significant concentrations of other toxic species, such as H_2S, CH_4 and GEM. The comparison between the chemical composition of punctual vents and soil diffuse gases revealed that secondary biogeochemical processes occurring at shallow depth (e.g. oxidation reaction, gas-water interaction and microbial activity) were able to strongly and efficiently affect the reduced gas species. Consequently, secondary processes play a key role in controlling the effective amounts of these species discharged into the atmosphere. Accordingly, whilst the total outputs of CO_2, H_2S and CH_4 from the study area were estimated in 2,660, 12 and 0.42 kg day^{-1}, respectively, the CO_2/H_2S and CO_2/CH_4 ratios of the gases diffusively released from the soil were significantly higher than those measured in gases from the punctual emissions (from 89 to 177 and from 1079 to 1,456, respectively). Our results indicated that the effective evaluation of the potential impact of air pollutants from deep gas reservoirs requires a complete geochemical survey on both diffuse and punctual emissions.

The air quality was estimated by a MMS approach, which produced a snapshot of the concentrations of the main deep-originated and by-product gas compounds along a pathway passing through the urban settlement mostly exposed to the lethal gases. Hydrogen sulfide was found to be the most impacting gas, producing odor annoyance up to more than 250 m from the emitting area and occasionally exceeding the 24-h air quality guideline for ambient air. High concentrations of CO_2, H_2S and CH_4 were also recorded in a poorly ventilated garage, likely due to gas permeation through the basement.

In the urban area of Cava dei Selci, the MMS survey coupled with a meteorological station allowed us to individuate the sites most prone to the deterioration of the air quality and provide useful information for deploying an early warning system based on gas monitoring through automated gas sensor network by the local authorities in order to avoid further lethal events and mitigate the potential hazard effects due the inhalation of toxic gases.

Acknowledgments

The sampling campaign at Cava dei Selci was performed in April 2016 in the framework of a field trip project ("*Studio multiparametrico sulle emissioni gassose naturali presso Cava dei Selci e Solfatara di Pomezia (Colli Albani, Roma): sviluppo di un protocollo di misura per la definizione di traccianti geochimici atti alla valutazione dell'impatto ambientale di aree affette da degassamento diffuso dal suolo*") partly sponsored by So.Ge.I.

(Italian Society of Geochemistry). Many thanks are due to local people for kindly providing their permission to perform air quality measurements inside their private garages and basements. We also thank Tullio Ricci and Giuseppe Etiope (National Institute of Geophysics and Volcanology INGV of Rome) for their help during the sampling session. The authors wish to thank the Associate Editor and two anonymous reviewers for their helpful comments that contributed to improve the first version of the manuscript.

Appendix A. Supplementary data

Supplementary data to this article can be found online at https://doi.org/10.1016/j.apgeochem.2019.01.003.

References

Amato, A., Chiarabba, C., 1995. Recent uplift of the Alban Hills volcano (Italy), evidence for magmatic inflation? Geophys. Res. Lett. 22, 1985–1988 1995.

Annunziatellis, A., Ciotoli, G., Lombardi, S., Nolasco, F., 2003. Short- and long-term gas hazard: the release of toxic gases in the Alban Hills volcanic area (central Italy). J. Geochem. Explor. 77, 93–108. https://doi.org/10.1016/S0375-6742(02)00272-8.

Arthur, C.L., Pawliszyn, J., 1990. Solid phase microextraction with thermal desorption using fused silica optical fibers. Anal. Chem. 62, 2145–2148.

Bagnato, E., Parello, F., Valenza, M., Caliro, S., 2009. Mercury content and speciation in the Phlegrean Fields volcanic complex: evidence from hydrothermal system and fumaroles. J. Volcanol. Geoth. Res. 187, 250–260. https://doi.org/10.1016/j.jvolgeores.2009.09.010.

Barbieri, M., Battistel, M., Boschetti, T., 2013. Chemical and isotope monitoring at Lake Albano (central Italy): water-rock interaction and climate change effects. Procedia Earth Planet. Sci. 7, 53–56. https://doi.org/10.1016/j.proeps.2013.03.117.

Beaubien, S.E., Ciotoli, G., Lombardi, S., 2003. Carbon dioxide and radon gas hazard in the Alban Hills area (central Italy). J. Volcanol. Geoth. Res. 123, 63–80. https://doi.org/10.1016/S0377-0273(03)00028-3.

Bernard, B.B., Brooks, J.M., Sackett, W.M., 1978. A geochemical model for characterization of hydrocarbon gas sources in marine sediments. Offshore Technology Conference 435–438 Houston, USA.

Cabassi, J., Tassi, F., Vaselli, O., Fiebig, J., Nocentini, M., Capecchiacci, F., Rouwet, D., Bicocchi, G., 2013. Biogeochemical processes involving dissolved CO_2 and CH_4 at Albano, Averno, and Monticchio meromictic volcanic lakes (Central-Southern Italy). Bull. Volcanol. 75, 683. https://doi.org/10.1007/s00445-012-0683-0.

Cabassi, J., Tassi, F., Venturi, S., Calabrese, S., Capecchiacci, F., D'Alessandro, W., Vaselli, O., 2017. A new approach for the measurement of gaseous elemental mercury (GEM) and H_2S in air from anthropogenic and natural sources: examples from Mt. Amiata (Siena, Central Italy) and Solfatara Crater (Campi Flegrei, Southern Italy). J. Geochem. Explor. 175, 48–58. https://doi.org/10.1016/j.gexplo.2016.12.017.

Camarda, M., De Gregorio, S., Favara, R., Gurrieri, S., 2007. Evaluation of carbon isotope fractionation of soil CO_2 under an advective-diffusive regimen: a tool for computing the isotopic composition of unfractionated deep source. Geochem. Cosmochim. Acta 71, 3016–3027. https://doi.org/10.1016/j.gca.2007.04.002.

Capasso, G., Favara, R., Inguaggiato, S., 1997. Chemical features and isotopic composition of gaseous manifestations on Vulcano Island (Aeolian Islands, Italy): an interpretative model of fluid circulation. Geochem. Cosmochim. Acta 61 (16), 3425–3440.

Capasso, G., D'Alessandro, W., Favara, R., Inguaggiato, S., Parello, F., 2001. Kinetic Isotope Fractionation of CO_2 Carbon Due to Diffusion Processes through the Soil. Water-Rock Interaction, vol. 10. Swets & Zeitlinger, Lisse, pp. 1497–1499.

Carapezza, M.L., Badalamenti, B., Cavarra, L., Scalzo, A., 2003. Gas hazard assessment in a densely inhabited area of Colli Albani Volcano (Cava dei Selci, Roma). J. Volcanol. Geoth. Res. 123, 81–94. https://doi.org/10.1016/S0377-0273(03)00029-5.

Carapezza, M.L., Tarchini, L., 2007. Accidental gas emission from shallow pressurized aquifers at Alban Hills volcano (Rome, Italy): geochemical evidence of magmatic degassing? J. Volcanol. Geoth. Res. 165, 5–16. https://doi.org/10.1016/j.jvolgeores.2007.04.008.

Carapezza, M.L., Lelli, M., Tarchini, L., 2008. Geochemistry of the Albano and Nemi crater lakes in the volcanic district of Alban hills (Rome, Italy). J. Volcanol. Geoth. Res. 178, 297–304. https://doi.org/10.1016/j.jvolgeores.2008.06.031.

Carapezza, M.L., Barberi, F., Tarchini, L., Ranaldi, M., Ricci, T., 2010. Volcanic hazards of the Colli Albani. In: Funiciello, R., Giordano, F. (Eds.), The Colli Albani Volcano. Geological Society of London, pp. 279–297.

Carapezza, M.L., Barberi, F., Ranaldi, M., Ricci, T., Tarchini, L., Barrancos, J., Fischer, C., Granieri, D., Lucchetti, C., Melian, G., Perez, N., Tuccimei, P., Vogel, A., Weber, K., 2012. Hazardous gas emissions from the flanks of the quiescent Colli Albani volcano (Rome, Italy). Appl. Geochem. 27, 1767–1782. https://doi.org/10.1016/j.apgeochem.2012.02.012.

Cardellini, C., Chiodini, G., Frondini, F., Granieri, D., Lewicki, J., Peruzzi, L., 2003. Accumulation chamber measurements of methane fluxes: application to volcanic-geothermal areas and landfills. Appl. Geochem. 18, 45–54.

Cardellini, C., Chiodini, G., Frondini, F., Avino, R., Bagnato, E., Caliro, S., Lelli, M., Rosiello, A., 2017. Monitoring diffuse volcanic degassing during volcanic unrests: the case of Campi Flegrei (Italy). Sci. Rep. 7 (1), 6757. https://doi.org/10.1038/s41598-017-06941-2.

Cataldi, R., Mongelli, F., Squarci, P., Taffi, L., Zito, G., Calore, C., 1995. Geothermal ranking of Italian territory. Geothermics 24, 115–129.

Cerling, T.E., Solomon, D.K., Quade, J., Bowman, J.R., 1991. On the isotopic composition of carbon in soil carbon dioxide. Geochem. Cosmochim. Acta 55 (11), 3403–3405. https://doi.org/10.1016/0016-7037(91)90498-T.

Chiodini, G., Cioni, R., Guidi, M., Raco, B., Marini, L., 1998. Soil CO_2 flux measurements in volcanic and geothermal areas. Appl. Geochem. 13 (5), 543–552.

Chiodini, G., Frondini, F., Kerrick, D.M., Rogie, J., Parello, F., Peruzzi, L., Zanzari, A.R., 1999. Quantification of deep CO_2 fluxes from Central Italy. Examples of carbon balance for regional aquifers and of soil diffuse degassing. Chem. Geol. 159, 205–222.

Chiodini, G., Frondini, F., Cardellini, C., Parello, F., Peruzzi, L., 2000. Rate of diffuse carbon dioxide Earth degassing estimated from carbon balance of regional aquifers: the case of central Apennine. Italy. J. Geophys. Res. 105 (B4), 8423–8434.

Chiodini, G., Frondini, F., 2001. Carbon dioxide degassing from the Albani Hills volcanic region. Central Italy. Chem. Geol. 177 97-83.

Chiodini, G., Cardellini, C., Amato, A., Boschi, E., Caliro, S., Frondini, F., Ventura, G., 2004. Carbon dioxide Earth degassing and seismogenesis in central and southern Italy. Geophys. Res. Lett. 31, L07615. https://doi.org/10.1029/2004GL019480.

Chiodini, G., 2008. A new web-based catalog of Earth degassing sites in Italy. Eos 89 (37), 341–342.

Chiodini, G., Cardellini, C., Caliro, S., Chiarabba, C., Frondini, F., 2013. Advective heat transport associated with regional Earth degassing in central Apennine (Italy). Earth Planet. Sci. Lett. 373, 65–74. https://doi.org/10.1016/j.epsl.2013.04.009.

Cinti, D., Procesi, M., Tassi, F., Montegrossi, G., Sciarra, A., Vaselli, O., Quattrocchi, F., 2011. Fluid geochemistry and geothermometry in the western sector of the Sabatini volcanic district and the Tolfa mountains (Central Italy). Chem. Geol. 284, 160–181. https://doi.org/10.1016/j.chemgeo.2011.02.017.

Cinti, D., Tassi, F., Procesi, M., Bonini, M., Capecchiacci, F., Voltattorni, N., Vaselli, O., Quattrocchi, F., 2014. Fluid geochemistry and geothermometry in the unexploited geothermal field of the Vicano-Cimino Volcanic District (Central Italy). Chem. Geol. 371, 96–114. https://doi.org/10.1016/j.chemgeo.2014.02.005.

Cinti, D., Tassi, F., Procesi, M., Brusca, L., Cabassi, J., Capecchiacci, F., Delgado Huertas, A., Galli, G., Grassa, F., Vaselli, O., Voltattorni, N., 2017. Geochemistry of hydrothermal fluids from the eastern sector of the Sabatini Volcanic District (Central Italy). Appl. Geochem. 84, 187–201. https://doi.org/10.1016/j.apgeochem.2017.06.014.

Cioni, R., Guidi, M., Raco, B., Marini, L., Gambardella, B., 2003. Water chemistry of lake Albano (Italy). J. Volcanol. Geoth. Res. 120, 179–195.

D'Alessandro, W., Brusca, L., Kyriakopoulos, K., Martelli, M., Michas, G., Papadakis, G., Salerno, F., 2011. Diffuse hydrothermal methane output and evidence of methanotrophic activity within the soils at Sousaki (Greece). Geofluids 11, 97–107. https://doi.org/10.1111/j.1468-8123.2010.00322.x.

Degens, E.T., 1969. Biogeochemistry of stable carbon isotopes. In: Eglington, G., Murphy, M.T.J. (Eds.), Organic Geochemistry. Springer, Berlin-Heidelberg-New York, pp. 194–208.

Denis, M.St, Song, X., Lu, J.Y., Feng, X., 2006. Atmospheric gaseous elemental mercury in downtown Toronto. Atmos. Environ. 40 (21), 4016–4024. https://doi.org/10.1016/j.atmosenv.2005.07.078.

Department of Health and Human Services (NIOSH), 2007. NIOSH Pocket Guide to Chemical Hazards. DHHS (NIOSH), Cincinnati, Ohio, pp. 424 Publication No. 2005-149.

Deutsch, C.V., Journel, A.G., 1998. GSLIB: Geostatistical Software Library and Users Guide. Oxford University Press, New York, pp. 1–369.

Di Filippo, M., Toro, B., 1995. Gravity features. Stratigraphy and volcano-tectonics. In: Trigila, R. (Ed.), The Volcano of the Alban Hills, Rome, pp. 213–219.

Di Martino, R.M.R., Capasso, G., Camarda, M., 2016. Spatial domain analysis of carbon dioxide from soils on Vulcano Island: implications for CO_2 output evaluation. Chem. Geol. 444, 59–70. https://doi.org/10.1016/j.chemgeo.2016.09.037.

Dubois, G., 2005. An Overview of Radon Survey in Europe. Radioactivity Environmental Monitoring Emissions and Health Unit Institute for Environment and Sustainability JRC. European Commission, pp. 168 EUR 21892 EN, EC.

Ebinghaus, R., Kock, H.H., Coggins, A.M., Spain, T.G., Jennings, S.G., Temme, C., 2002. Long-term measurements of atmospheric mercury at Mace Head, Irish west coast, between 1995 and 2001. Atmos. Environ. 36, 5267–5276. https://doi.org/10.1016/S1352-2310(02)00691-X.

Esbrí, J.M., Martínez-Coronado, A., Higueras, P.L., 2016. Temporal variations in gaseous elemental mercury concentrations at a contaminated site: main factors affecting nocturnal maxima in daily cycles. Atmos. Environ. 125 (A), 8–14. https://doi.org/10.1016/j.atmosenv.2015.10.064.

Evans, W.C., White, L.D., Rapp, J.B., 1998. Geochemistry of some gases in hydrothermal fluids from the southern Juan de Fuca ridge. J. Geophys. Res. 15, 305–313.

Federico, C., Corso, P.P., Fiordilino, E., Cardellini, C., Chiodini, G., Parello, F., Pisciotta, A., 2010. CO_2 degassing at La Solfatara volcano (Phlegrean Fields): processes affecting $\delta^{13}C$ and $\delta^{18}O$ of soil CO_2. Geochem. Cosmochim. Acta 74, 3521–3538. https://doi.org/10.1016/j.gca.2010.03.010.

Fitzgerald, W., Lamborg, C., 2007. Geochemistry of mercury in the environment. In: Holland, H., Turekian, K. (Eds.), Environmental Geochemistry, Treatise on Geochemistry. Elsevier, pp. 1–47.

Frepoli, A., Amato, A., 1997. Contemporaneous extension and compression in the Northern Apennines from earthquake fault-plane solutions. Geophys. J. Int. 129, 368–388.

Frondini, F., Chiodini, G., Caliro, S., Cardellini, C., Granieri, D., Ventura, G., 2004. Diffuse CO_2 degassing at Vesuvio. Italy. Bull. Volcanol. 66, 642–651. https://doi.org/10.1007/s00445-004-0346-x.

Fu, X.W., Feng, X., Dong, Z.Q., Yin, R.S., Wang, J.X., Yang, Z.R., Zhang, H., 2010. Atmospheric gaseous elemental mercury (GEM) concentrations and mercury depositions at a high-altitude mountain peak in south China. Atmos. Chem. Phys. 10, 2425–2437.

Gagliano, A.L., D'Alessandro, W., Tagliavia, M., Parello, F., Quatrini, P., 2014. Methanotrophic activity and diversity of methanotrophs in volcanic geothermal soils at Pantelleria (Italy). Biogeosciences 11, 5865–5875. https://doi.org/10.5194/bg-11-5865-2014.

Gellhorn, E., 1936. The effect of O_2-lack, variations in the CO_2-content of the inspired air, and hyperpnea on visual intensity discrimination. Am. J. Physiol. 115, 679–684.

Giggenbach, W.F., Gonfiantini, R., Jangi, B.L., Truesdell, A.H., 1983. Isotopic and chemical composition of Parbati valley geothermal discharges, north-west himalaya, India. Geothermics 12 (2/3), 199–222.

Giggenbach, W.F., Minissale, A.A., Scandiffio, G., 1988. Isotopic and chemical assessment of geothermal potential of the Colli Albani area, Latium region. Italy. Appl. Geochem. 3, 475–486.

Giggenbach, W.F., 1991. Chemical techniques in geothermal exploration. In: D'Amore, F. (Ed.), Application of Geochemistry in Geothermal Reservoir Development. UNITAR, Rome, pp. 119–144.

Giggenbach, W.F., 1996. Chemical composition of volcanic gases. In: Scarpa, R., Tilling, R. (Eds.), Monitoring and Mitigation of Volcano Hazards. Springer, Berlin, pp. 221–256.

Giordano, G., De Benedetti, A.A., Diana, A., Diano, G., Gaudioso, F., Marasco, F., Miceli, M., Mollo, S., Cas, R.A.F., Funiciello, R., 2006. The Colli Albani mafic caldera (Roma, Italy): Stratigraphy, structure and petrology. J. Volcanol. Geoth. Res. 155, 49–80. https://doi.org/10.1016/j.jvolgeores.2006.02.009.

Giordano, G., De Benedetti, A.A., Bonamico, A., Ramazzotti, P., Mattei, M., 2014. Incorporating surface indicators of reservoir permeability into reservoir volume calculations: application to the Colli Albani caldera and the Central Italy Geothermal Province. Earth Sci. Rev. 128, 75–92. https://doi.org/10.1016/j.earscirev.2013.10.010.

Glamoclija, M., Garrel, L., Berthon, J., López-García, P., 2004. Biosignatures and bacterial diversity in hydrothermal deposits of Solfatara crater. Italy. Geomicrobiol. J. 21, 529–541. https://doi.org/10.1080/01490450490888235.

Grassa, F., Capasso, G., Oliveri, Y., Sollami, A., Carreira P Carvalho, M.R., Marques, J.M., Nunes, J.C., 2010. Nitrogen isotopes determination in natural gas: analytical method and first results on magmatic, hydrothermal and soil gas samples. Isot. Environ. Health Stud. 46, 141–155. https://doi.org/10.1080/10256016.2010.491914.

Harkness, J.S., Darrah, T.H., Warner, N.R., Whyte, C.J., Moore, M.T., Millot, R., Kloppmann, W., Jackson, R.B., Vengosh, A., 2017. The geochemistry of naturally occurring methane and saline groundwater in an area of unconventional shale gas development. Geochem. Cosmochim. Acta 208, 302–334. https://doi.org/10.1016/j.gca.2017.03.039.

Henson, J., Redman, R., Rodriguez, R., Stout, R., 2005. Fungi in Yellowstone's geothermal soils and plants. Yellowstone Science 13 (4), 25–30.

Hilton, D.R., Fischer, T.P., Marty, B., 2002. Noble gases and volatile recycling at subduction zones. In: In: Porcelli, D., Ballentine, C.J., Wieler, R. (Eds.), Noble Gases in Cosmochemistry and Geochemistry. Rev. Mineral, vol. 47. pp. 319–370 1.

Hooker, P.J., Bertrami, R., Lombardi, S., O'Nions, R.K., Oxburgh, E.R., 1985. Helium-3 anomalies and crust–mantle interaction in Italy. Geochem. Cosmochim. Acta 49, 2505–2513.

Huber, R., Sacher, M., Vollmann, A., Huber, H., Rose, D., 2000. Respiration of arsenate and selenate by hyperthermophilic Archaea. System. Appl. Microbiol. 23, 305–314.

Iacono Marziano, G., Gaillard, F., Pichavant, M., 2007. Limestone assimilation and the origin of CO_2 emissions at the Alban Hills (Central Italy): constraints from experimental petrology. J. Volcanol. Geoth. Res. 166 (2), 91–105. https://doi.org/10.1016/j.jvolgeores.2007.07.001.

Kolb, C.E., Herndon, S.C., McManus, J.B., Shorter, J.H., Zahniser, M.S., Nelson, D.D., Jayne, J.T., Canagaratna, M.R., Worsnop, D.R., 2004. Mobile laboratory with rapid response instruments for real-time measurements of urban and regional trace gas and particulate distributions and emission source characteristics. Environ. Sci. Technol. 38, 5694–5703. https://doi.org/10.1021/es030718p.

Langford, N.J., 2005. Carbon dioxide poisoning. Toxicol. Rev. 24, 229–235.

Laville, P., Neri, S., Continanza, D., Ferrante Vero, L., Bosco, S., Virgili, G., 2015. Cross-validation of a mobile N_2O flux prototype (IPNOA) using micrometeorological and chamber methods. JEPE 9, 375–385. https://doi.org/10.17265/1934-8975/2015.04.007.

Mariucci, M.T., Amato, A., Montone, P., 1999. Recent tectonic evolution and present stress in the Northern Apennines (Italy). Tectonics 18 (1), 108–118.

Marra, F., Gaeta, M., Giaccio, B., Jicha, B.R., Palladino, D.M., Polcari, M., Sottili, G., Taddeucci, J., Florindo, F., Stramondo, S., 2016. Assessing the volcanic hazard for Rome: $^{40}Ar/^{39}Ar$ and In-SAR constraints on the most recent eruptive activity and present-day uplift at Colli Albani Volcanic District. Geophys. Res. Lett. 43, 6898–6906. https://doi.org/10.1002/2016GL069518.

Martelli, M., Nuccio, P.M., Stuart, F.M., Burgess, R., Ellam, R.M., Italiano, F., 2004. Helium–strontium isotope constraints on mantle evolution beneath the Roman Comagmatic Province, Italy. Earth Planet. Sci. Lett. 224, 295–308. https://doi.org/10.1016/j.epsl.2004.05.025.

Martrette, J.M., Egloff, C., Clément, C., Yasukawa, K., Thornton, S.N., Trabalon, M., 2017. Effects of prolonged exposure to CO_2 on behavior, hormone secretion and respiratory muscles in young female rats. Physiol. Behav. 177, 257–262. https://doi.org/10.1016/j.physbeh.2017.05.007.

Marty, B., Zimmermann, L., 1999. Volatiles (He, C, N, Ar) in mid-ocean ridge basalts: assessment of shallow-level fractionation and characterization of source composition. Geochem. Cosmochim. Acta 63, 3619–3633.

Mattei, M., Conticelli, S., Giordano, G., 2010. The Tyrrhenian margin geological setting: from the Apennine orogeny to the K-rich volcanism. In: In: Funiciello, R., Giordano, G. (Eds.), The Colli Albani Volcano, vol. 3. Special Publications of IAVCEI, pp. 7–27.

McCollom, T.M., Seewald, J.S., 2007. Abiotic synthesis of organic compounds in deep-sea hydrothermal environments. Chem. Rev. 107, 382–401. https://doi.org/10.1021/cr0503660.

Minissale, A., Evans, W.C., Magro, G., Vaselli, O., 1997. Multiple source components in gas manifestations from north-central Italy. Chem. Geol. 142, 175–192.

Minissale, A., 2004. Origin, transport and discharge of CO_2 in central Italy. Earth Sci. Rev. 66, 89–141. https://doi.org/10.1016/j.earscirev.2003.09.001.

Montegrossi, G., Tassi, F., Vaselli, O., Buccianti, A., Garofalo, K., 2001. Sulphur species in volcanic gases. Anal. Chem. 73, 3709–3715. https://doi.org/10.1021/ac001429b.

Moore, M.T., Vinson, D.S., Whyte, C.J., Eymold, W.K., Walsh, T.B., Darrah, T.H., 2018. Differentiating between biogenic and thermogenic sources of natural gas in coalbed methane reservoirs from the Illinois Basin using noble gas and hydrocarbon geochemistry. Geol. Soc. London Spec. Publ. 468, 151–188. https://doi.org/10.1144/SP468.8.

NIOSH, 1996. Documentation for immediately dangerous to life or health concentrations (IDLHs) for carbon dioxide. Available at: http://www.cdc.gov/niosh/idlh/124389.html.

NIST, 2005. NIST/EPA/NIH mass spectral library, 2005. web site. http://www.nist.gov/srd/nist1a.htm.

Norris, T.B., Wraith, J.M., Castenholz, R.W., McDermott, T.R., 2002. Soil microbial community structure across a thermal gradient following a geothermal heating event. Appl. Environ. Microbiol. 68 (12), 6300–6309. https://doi.org/10.1128/AEM.68.12.6300–6309.2002.

Olafsdottir, S., Gardarsson, S.M., Andradottir, H.O., 2014. Natural near field sinks of hydrogen sulfide from two geothermal power plants in Iceland. Atmos. Environ. 96, 236–244.

Orlando, A., Conticelli, S., Manetti, P., Vaggelli, G., 1994. The basement of northern Vulsinian volcanic District as inferred from the study of crustal xenoliths from the Torre Alfina lavas, Viterbo, central Italy. Mem. Soc. Geol. It. 48, 681–688.

Ozima, M., Podosek, F.A., 2002. Noble Gas Geochemistry, second ed. Cambridge University Press, Cambridge 286.

Paonita, A., Caracausi, A., Iacono-Marziano, G., Martelli, M., Rizzo, A., 2012. Geochemical evidence for mixing between fluids exsolved at different depths in the magmatic system of Mt Etna (Italy). Geochem. Cosmochim. Acta 84, 380–394. https://doi.org/10.1016/j.gca.2012.01.028.

Peccerillo, A., 1999. Multiple mantle metasomatism in central-southern Italy: geochemical effects, timing and geodynamic implications. Geology 27, 315–318.

Peccerillo, A., 2005. Plio-Quaternary Volcanism in Italy. Petrology, Geochemistry, Geodynamics. Springer, Heidelberg 365.

Peralta, O., Castro, T., Durón, M., Salcido, A., Celada-Murillo, A.T., Navarro-González, R., Márquez, C., García, J., de la Rosa, J., Torres, R., Villegas-Martínez, R., Carreón-Sierra, S., Imaz, M., Martínez-Arroyo, A., Saavedra, I., de la Luz, E.M., Torres-Jaramillo, A., 2013. H_2S emissions from Cerro Prieto geothermal power plant, Mexico, and air pollutants measurements in the area. Geothermics 46, 55–65.

Petruzzi, S., Musi, B., Bignami, G., 1994. Acute and chronic sulphur dioxide (SO_2) exposure: an overview of its effects on humans and laboratory animals. Ann. Ist. Super Sanita 30 (2), 151–156.

Pizzino, L., Galli, G., Mancini, C., Quattrocchi, F., Scarlato, P., 2002. Natural gas hazard (CO_2, ^{222}Rn) within a quiescent volcanic region and its relations with tectonics: the case of the *Ciampino-Marino* area, Alban hills volcano, Italy. Nat. Hazards 27, 257–287.

Rogie, J.D., Kerrick, D.M., Chiodini, G., Frondini, F., 2000. Flux measurements of non-volcanic CO_2 emission from some vents in central Italy. J. Geophys. Res. 105 (B4), 8435–8445.

Rojo, F., 2009. Degradation of alkanes by bacteria. Environ. Microbiol. 11 (10), 2477–2490. https://doi.org/10.1111/j.1462-2920.2009.01948.x.

Rollinson, H., 1993. Using Geochemical Data. Longman, London, UK 352.

Sano, Y., Marty, B., 1995. Origin of carbon in fumarolic gas from island arcs. Chem. Geol. 119, 265–274.

Schroeder, W.H., Munthe, J., 1998. Atmospheric mercury—an overview. Atmos. Environ. 32, 809–822.

Scripps CO_2 Program, Scripps institution of oceanography UC san Diego, http://scrippsco2.ucsd.edu.

Scrocca, D., Doglioni, C., Innocenti, F., 2003. Constraints for an interpretation of the Italian geodynamics: a review. Mem. Descr. Carta Geologica d'It. 62, 15–46.

Sechzer, P.H., Egbert, L.D., Linde, H.W., Cooper, D.Y., Dripps, R.D., Price, H.L., 1960. Effect of CO_2 inhalation on arterial pressure, ECG and plasma catecholamines and 17-OH corticosteroids in normal man. J. Appl. Physiol. 15, 454–458.

Sholupov, S.E., Ganeyev, A.A., 1995. Zeeman atomic absorption spectrometry using high frequency modulated light polarization. Spectrochim. Acta B At. Spectrosc. 50, 1227–1236.

Sholupov, S., Pogarev, S., Ryzhov, V., Mashyanov, N., Stroganov, A., 2004. Zeeman atomic absorption spectrometer RA-915+ for direct determination of mercury in air and complex matrix samples. Fuel Process. Technol. 85, 473–485.

Sinclair, A.J., 1974. Selection of threshold values in geochemical data using probability graphs. J. Geochem. Explor. 3, 129–149.

Sommar, J., Gårdfeldt, K., Strömberg, D., Feng, X., 2001. A kinetic study of the gas-phase reaction between the hydroxyl radical and atomic mercury. Atmos. Environ. 35, 3049–3054.

Taran, Y., 2011. N_2, Ar, and He as a tool for discriminating sources of volcanic fluids with application to Vulcano. Italy. Bull. Volcanol. 73, 395–408. https://doi.org/10.1007/s00445-011-0448-1.

Tassi, F., Vaselli, O., Cuccoli, F., Buccianti, A., Nisi, B., Lognoli, E., Montegrossi, G., 2009. A geochemical multi-methodological approach in hazard assessment of CO_2-rich gas emissions at Mt. Amiata volcano (Tuscany, Central Italy). Water Air Soil Pollut. Focus 9 (1–2), 117–127. https://doi.org/10.1007/s11267-008-9198-2.

Tassi, F., Fiebig, J., Vaselli, O., Nocentini, M., 2012. Origins of methane discharging from volcanic-hydrothermal emissions in Italy. Chem. Geol. 310–311, 36–48. https://doi.

org/10.1016/j.chemgeo.2012.03.018.
Tassi, F., Nisi, B., Cardellini, C., Capecchiacci, F., Donnini, M., Vaselli, O., Avino, R., Chiodini, G., 2013. Diffuse soil emission of hydrothermal gases (CO_2, CH_4, C_6H_6) at Solfatara crater (Campi Flegrei, southern Italy). Appl. Geochem. 35, 142–153. https://doi.org/10.1016/j.apgeochem.2013.03.020.
Tassi, F., Venturi, S., Cabassi, J., Capecchiacci, F., Nisi, B., Vaselli, O., 2015a. Volatile organic compounds (VOCs) in soil gases from Solfatara crater (Campi Flegrei, southern Italy): Geogenic source(s) vs. biogeochemical processes. Appl. Geochem. 56, 37–49. https://doi.org/10.1016/j.apgeochem.2015.02.005.
Tassi, F., Venturi, S., Cabassi, J., Vaselli, O., Gelli, I., Cinti, D., Capecchiacci, F., 2015b. Biodegradation of CO_2, CH_4 and volatile organic compounds (VOCs) in soil gas from the Vicano-Cimino hydrothermal system (central Italy). Org. Geochem. 86, 81–93. https://doi.org/10.1016/j.orggeochem.2015.06.004.
Thermo Fisher Scientific Inc, 2012. Thermo Scientific model 450i hydrogen sulfide & sulfur dioxide analyzer manual. https://www.thermoscientific.com/content/dam/tfs/ATG/EPD/EPD%20Documents/Product%20Manuals%20&%20Specifications/Air%20Quality%20Instruments%20and%20Systems/Ambient%20Gas/D19731~.pdf.
Thi Nguyen, H., Kim, K.H., Ma, C.J., Cho, S.J., Ryeul Sohn, J., 2010. A dramatic shift in CO and CH_4 levels at urban locations in Korea after the implementation of the Natural Gas Vehicle Supply (NGVS) program. Environ. Res. 110 (4), 396–409. https://doi.org/10.1016/j.envres.2010.03.002.
Trasatti, E., Marra, F., Polcari, M., Etiope, G., Ciotoli, G., Darrah, T.H., Tedesco, D., Stramondo, S., Florindo, F., Ventura, G., 2018. Coeval uplift and subsidence reveal magma recharging near Rome (Italy). Geochem. Geophys. Geosyst. 19, 1484–1498. https://doi.org/10.1029/2017GC007303.
Trigila, R., Agosta, E., Currado, C., De Benedetti, A.A., Freda, C., Gaeta, M., Palladino, D.M., Rosa, C., 1995. Petrology. In: Trigila, R. (Ed.), The Volcano of the Alban Hills. Tipografia S.G.S., Roma, pp. 95–165.
Tunnicliffe, W.S., Hilton, M.F., Harrison, R.M., Ayres, J.G., 2001. The effect of sulphur dioxide exposure on indices of heart rate variability in normal and asthmatic adults. Eur. Respir. J. 17 (4), 604–608.
USEPA, 1997. Mercury Study Report to Congress. EPA-452/R-97-005. Fate and Transport of Mercury in the Environment III. U.S. Environmental Protection Agency.
Vaselli, O., Tassi, F., Montegrossi, G., Capaccioni, B., Giannini, L., 2006. Sampling and analysis of volcanic gases. Acta Vulcanol. 18 (1–2), 65–76.
Vaselli, O., Nisi, B., Tassi, F., Rappuoli, D., Pancioli, V., Ucciero, S., Giannini, L., 2011. CO_2 hazard vs touristic attraction at the Mt. Amiata volcano (Italy). Acta Vulcanol. 23 (1–2), 71–78.
Whiticar, M.J., 1999. Carbon and hydrogen isotope systematics of bacterial formation and oxidation of methane. Chem. Geol. 161, 291–314.
WHO, 2000. Air Quality Guidelines for Europe, second ed. WHO Regional Publications European Series, No. 91.
WHO, 2003. Hydrogen Sulfide: Human Health Aspects. Concise International Chemical Assessment Document 53. World Health Organization, Geneva, Switzerland.
WHO, 2006. Air Quality Guidelines for Particulate Matter, Ozone, Nitrogen Dioxide and Sulfur Dioxide. Global Update 2005. Summary of Risk Assessment. World Health Organization 2006. http://www.who.int/phe/health_topics/outdoorair/outdoorair_aqg/en/.
Worden, R.H., Smalley, P.C., 1996. H_2S-producing reactions in deep carbonate gas reservoirs: Khuff Formation, Abu Dhabi. Chem. Geol. 133, 157–171.